ISSN 1288-1619

CNRS - Université Pierre et Marie Curie - Université Versailles-Saint-Quentin
CEA - ORSTOM - Ecole Normale Supérieure - Ecole Polytechnique

Institut Pierre Simon Laplace
des Sciences de l'Environnement Global

Notes du Pôle de Modélisation

Sensitivity of Photochemical Pollution using the Adjoint of a Simplified Chemistry-Transport Model

L. Menut (1), R. Vautard (1), C. Honnoré (1), M. Beekmann (2)

(1) IPSL - Laboratoire de Météorologie Dynamique;
(2) IPSL - Service d'Aéronomie

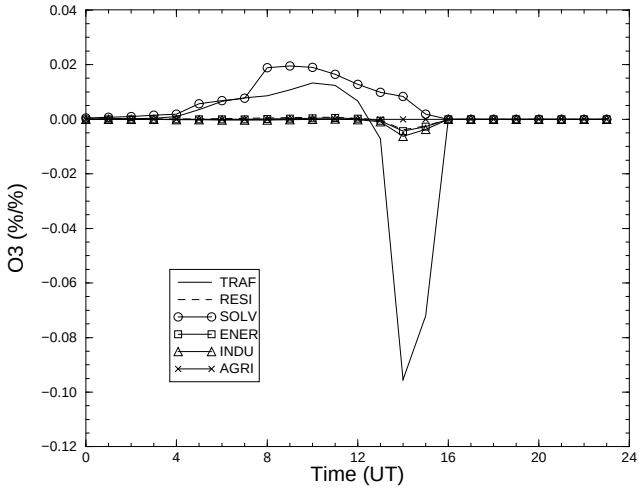

Décembre 1999 **Note n° 15**

I P S L

CNRS - Université Pierre et Marie Curie - Université Versailles-Saint-Quentin
CEA -CNES - ORSTOM - Ecole Normale Supérieure - Ecole Polytechnique

Institut Pierre Simon Laplace
des Sciences de l'Environnement Global

CETP - LMD - LODYC - LPCM - LSCE - SA

Université Pierre-et-Marie-Curie
B 102 - T15-E5 - 4, Place Jussieu
75252 Paris Cedex 05 (France)
Tél : (33) 01 44 27 39 83
Fax : (33) 01 44 27 37 76

Université Versailles-Saint-Quentin
College Vauban, 47 Boulevard Vauban
78047 Guyancourt Cedex (France)
Tél : (33) 01 39 25 58 17
Fax : (33) 01 39 25 58 22

Sensitivity of Photochemical Pollution using the Adjoint of a Simplified Chemistry-Transport Model

L. Menut (1), R. Vautard (1), C. Honnoré (1), M. Beekmann (2)

(1) IPSL - Laboratoire de Météorologie Dynamique;
(2) IPSL - Service d'Aéronomie

Deux épisodes de forte pollution atmosphérique estivale en région Parisienne sont étudies par modélisation adjointe. Le premier épisode (12 Juillet 1994) est typique d'un événement de pollution 'localement produite' par la ville, alors que le second (12 Aout 1997) est principalement dû à l'advection de hautes concentrations d'ozone sur la région parisienne. Nous calculons, á l'aide de l'adjoint d'un modèle de chimie-transport simplifié, les sensibilités des pics de polluants aux émissions surfaciques et aux taux de réactions chimiques du mécanisme employé. La sensibilité aux émissions montre tout d'abord que le premeir épisode est essentiellement sensible aux émissions de composés organiques volatils (COVs), alors que le second est plus sensible aux émissions de NO_x. Ces résultats mettent en avant les deux secteurs les plus importants: le trafic automobile et les solvants industriels. La sensibilité aux taux de réactions montre que la production oxydante n'est sensible qu'à quelques réactions du mécanisme. La très forte sensibilité à certaines d'entre elles mettent en avant le besoin d'approfondir nos connaissances sur certains taux de réactions chimiques encore très incertains.

Décembre 1999
Note n° 15

Directeur de publication : Gérard Mégie, Directeur de l'IPSL
ISSN 1288-1619

Sensitivity of Photochemical Pollution using the Adjoint of a Simplified Chemistry-Transport Model

L. Menut, R. Vautard, C. Honoré
Institut Pierre Simon Laplace - Laboratoire de Météorologie Dynamique,
Ecole Polytechnique, Palaiseau, France

M. Beekmann
Institut Pierre Simon Laplace - Service d'Aéronomie,
Université P.M. Curie, Paris, France

Abstract

The nature of two summertime photooxidant pollution episodes over Paris is investigated by means of adjoint modeling. The first episode (July 12, 1994) is characteristic of a 'local production' episode, while the second (August 12, 1997) is mostly due to advection into the urban area of high concentrations of ozone. We calculate the sensitivities to emissions of individual primary species and to reaction rate coefficients using the adjoint of a simplified multibox model representing the urban and suburban areas of the city of Paris. Sensitivity to emissions demonstrates that the first episode is essentially sensitive to volatile organic compounds (VOC)/NO_x emissions, while the second is sensitive to NO_x emissions. These results also point out the two important emission activity categories: traffic and solvent use, the second one being more sensitive than the first one. Sensitivity to reaction rates indicates that oxidant production is only sensitive to a few reactions. The high sensitivity of photochemical pollutants peaks to particular chemical reactions points out the necessity to refine the knowledge of their reaction rates.

1 Introduction

Air quality management in urban areas has become, over the last few decades, a major problem for decision makers. In some critical areas and for some pollutants, atmospheric concentrations have undergone a drastic decrease, due to adequate emission regulations. However, the relationship between emissions and atmospheric concentrations can be obscured by the nonlinear character of chemical transformations. Such is the case of the problem of ozone level reduction in urban and suburban areas. Recent articles and reports show indeed that the impact of regulations on ozone levels can be quite weak [*Strand and Hov*, 1994; *Bruckmann and Wichmann-Fiebig*, 1997; *Vautard et al.*, 1998]. The same problem probably occurs for air pollution by aerosols, since they are formed both by direct emissions and by gas-particle conversions.

The key question is to determine the sensitivity of pollutant concentrations to emissions of individual pollutants. In practical terms this means to determine the sensitivity of pollutant concentrations to a reduction of emissions of given emission categories (traffic, point sources, etc...) at given times and locations.

The problem of sensitivity of air pollutant concentrations to other factors (meteorology, chemical reaction rates, etc...) addresses many research questions that are not necessarily of major concern for decision makers, but however are fundamental to our understanding of the physical and chemical mechanisms of air pollution.

Most of the sensitivity questions are left to modelers since the experimental approach is difficult and expensive at the scale of a city. The traditional approach to sensitivity consists

in performing "twin simulations" with one parameter perturbed. While this method is quite efficient in determining the impact of regulations of a few control parameters, it generally requires too many simulations when the local (in space or time) character of sensitivity is addressed. For instance, assume that one wants to determine the sensitivity of a pollutant concentration to the reduction of emissions in each individual three-dimensional (3-D) model grid cell; this would require a control simulation and as many sensitivity simulations as grid cells.

Thus direct modeling can not address all sensitivity issues. Some recent studies use automatic differentiation [*Carmichael et al.*, 1997] or the 'direct decoupled method' [*Gao et al.*, 1995; *Seefeld and Stockwell*, 1999] to retrieve sensitivity of ozone to initial conditions or to time-dependent rate parameters. In this paper we propose a complementary approach, based on adjoint modeling, that could be used for the kind of problems mentioned above. The aim of the adjoint of a simulation model is to calculate the gradients $\partial c/\partial p_i$ of a scalar quantity c to a collection of N parameters $(p_i, i = 1, N)$ at the cost of a few direct simulations. The development of adjoint models was initially proposed in a simplified context by *Marchuk* [1974] and more theoretically developed by *Lewis and Derber* [1985] and *Talagrand and Courtier* [1987] within the context of meteorological data assimilation. Adjoint models are now widely used, for instance in the operational setting of 4D-VAR assimilation of European Center at Medium-range Weather Forecasts [*Filiberti et al.*, 1998], or in sensitivity studies in the context of the NCEP Medium-range Weather Forecasts [*Li and Navon*, 1998], and air quality [*Gao et al.*, 1995]. Recently, idealized experiments of chemical data assimilations have been performed [*Elbern et al.*, 1997; *Elbern and Schmidt*, 1999], using the EURAD chemistry-transport model and its adjoint. The adjoint model can also be used for inverse modeling of boundary conditions, such as demonstrated by *Vautard et al.*, [1998]. However, as far as we know, the adjoint of a chemistry-transport model has never been used for determining sensitivities of air pollutants to emissions and other parameters.

We propose here the application of the adjoint of a simplified urban photochemical model to the determination of the sensitivity of two summer photochemical episodes (July 12, 1994 and August 12, 1997) to various parameters, including emissions, over the urban area of Paris and its suburbs. We examine in particular the sensitivity of the ozone and nitrogen dioxyde peak concentrations, which were quite high for both days (about 100 ppb for ozone), to both categorized and individual pollutant emissions and chemical reaction rates.

In section 2 we describe the model used. Section 3 is devoted to the description of two case studies. Sections 4 and 5 present respectively the results of sensitivity to emissions and reaction rates.

2 The model and the adjoint formulation

2.1 Model general formulation

2.1.1 Model geometry

The purpose of this paper being mostly methodological, we use, throughout this paper, a simplified urban chemistry-transport model, CHIMERE. The model formulation consists of a somewhat more realistic adaptation of the box model approach proposed by *Jin and Demerjian* [1993]. Our aim is not to represent the detailed wind circulations and pollutant fields at small scale, but rather to model the urban chemistry-transport problem at the

scale of a big city in a qualitatively correct manner.

The city of Paris and its surroundings clearly calls for such a simplified representation, since it is located in a plain area, and the urban structure is mostly concentrated in the center with rural areas almost all around.

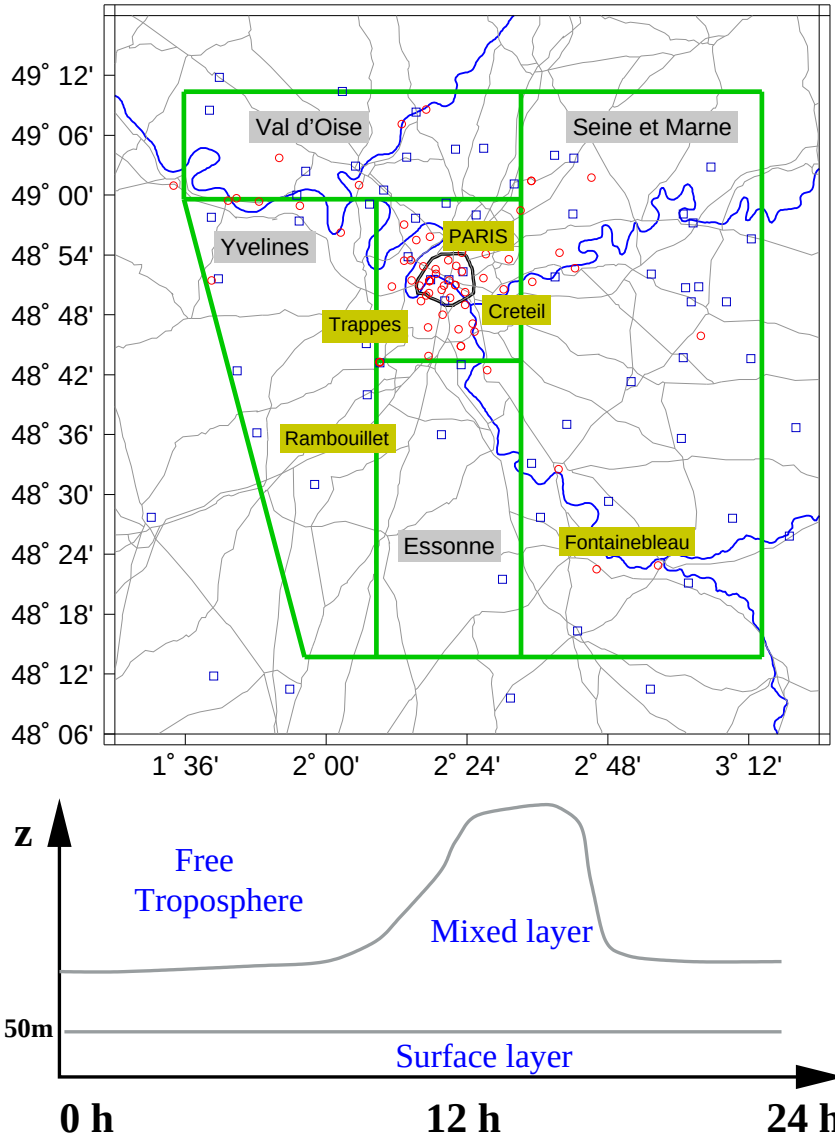

Figure 1: *Principle of the CHIMERE geometry for the Paris area. The city of Paris is located at the center of the map (top). The five boxes defined for the model are represented with the bold solid lines, including the name of the area: 'Paris' for the urban box, 'Val d'Oise', 'Yvelines', Essonne' and 'Seine et Marne' for the suburban boxes, with the cities of Creteil, Fontainebleau and Rambouillet. Only two vertical layers are taken into account in the calculation: the surface layer, with a constant height of 50m, and the mixed layer, with a diurnal height evolution (bottom).*

To account for this structure, the model domain, displayed in Figure 1, is divided horizontally into five boxes. The central box represents the most urbanized area (Paris and the "Petite Couronne"), while the other four boxes represent suburban and rural

administrative districts. This geometrical choice is motivated by its compatibility with the emissions database, provided as totals within these districts. While the boundaries of the districts remain approximate, their surfaces are exact, in order not to overestimate or underestimate average surface sources.

It is noteworthy that the city pollution plume cannot be correctly simulated by the model, due to the fairly large external box sizes of the model. In fact, these external boxes are only used for providing species concentrations at the boundaries of the central domain. As these boxes only played a boundary role (dynamical and chemical, including surface emissions), the results, thoughout this paper, are only considered within the central box: the urban box.

Along the vertical, the model represents the boundary layer, divided into a surface layer of constant height h_s=50 m and a mixed layer of variable thickness $\overline{h}$. Mixing is assumed between the two model layers and air from above is entrained into the mixed layer during its growth in early morning to mid afternoon.

2.1.2 Meteorological forcing

One of our main motivations in the construction of this model is actually to forecast daily concentration maxima. In view of this application, which will be described in a future article, the model has to be forced by routinely available meteorological analyses and forecasts. In the present paper, the model is entirely forced by the local values (over the "Paris grid point") of European Centre for Medium-Range Forecasts (ECMWF) first guesses (6-hour forecasts). This choice, instead of using analyses, is motivated by the lack, or erroneous structure, of some necessary variables (mainly cloudiness) in the ECMWF analyses.

Owing to the simplified character of the model, and the large-scale nature of meteorological input data, all the meteorological variables used are assumed to be horizontally homogeneous, but layer and time dependent over the model domain. As meteorological forcing, the model requires (1) wind values (u and v) in each layer, used for horizontal transport, (2) temperature (T), used for the calculation of chemical reaction rates, (3) specific humidity (q), used for chemistry, (4) air density (ρ), also used for chemistry, (5) cloudiness (n) , used for the attenuation of photolysis rates, and (6) boundary layer height ($\overline{h}$).

The first four variables are calculated by averaging ECMWF data within the two model layers. They are originally provided with a 6-hour frequency, and they must undergo a time interpolation (splines) in order to obtain hourly values.

The calculation of the boundary layer height is based on the geometry of the potential temperature profile. It is the height $\overline{h}$ at which potential temperature $\theta(z = \overline{h})$ reaches the value of potential temperature at some reference altitude $\theta(z_0)$ (z_0=50 m), plus an extra temperature departure θ', in order to account for the thermal extra temperature near ground level. In order to smooth out occasional irregularities of the potential temperature profile, the height is estimated for 100 values of θ', drawn from an exponential distribution with an average of 1^o, and the mean height is taken for input to the CHIMERE model.

2.1.3 Chemistry-transport budget equation

Within each model box, the evolution equation of species concentrations $C(t)$ is taken as its flux budget:

$$\frac{\partial C}{\partial t} = F_h^+ + F_m^+ + F_c^+ + F_e^+ - F_h^- - F_m^- - F_c^- - F_d^-,$$

where superscripts ($^+$) and ($^-$) denote the production and loss fluxes, respectively. Subscript h stands for horizontal transport, m for mixing and entrainment, c for chemistry, e for emissions, and d for dry deposition.

2.2 Physical Parameterizations

2.2.1 Horizontal transport

Within each model box, horizontal advection fluxes F_h^+ and F_h^- are calculated from the upstream formulae:

$$F_h^+ = \frac{1}{S}\sum_k l_k V_k C_k \qquad F_h^- = \frac{1}{S}\sum_{k'} l_{k'} V_{k'} C,$$

where the two above sums run on adjacent upstream and downstream boxes, respectively C_k are the corresponding upstream concentrations, V_k and $V_{k'}$ are the components of the wind field normal to the interfaces, l_k and $l_{k'}$ are the lengths of these interfaces, and S is the box surface. This upstream advection scheme, of first order, is particularly well suited in the case of an irregular mesh such as in the present model.

2.2.2 Vertical mixing and entrainment

Again for the sake of simplicity, mixing between the surface layer and the mixed layer is taken as a diffusion of species between them. In the surface layer this parametrization leads to

$$F_m^+ = k(\overline{h})\frac{C_{\text{mix}}}{h_s} \qquad F_m^- = k(\overline{h})\frac{C_{\text{surf}}}{h_s},$$

where $k(\overline{h})$ (m^2s^{-1}) is the diffusion coefficient, assumed to depend only on $\overline{h}$. Such a parameterization is reasonable during convective hours, but does not account for mechanical turbulent fluxes. An empirical formula is chosen for $k(\overline{h})$:

$$k(\overline{h}) = a + b\overline{h}$$

where $a = 0.4\ \text{m}^2\text{s}^{-1}$ and $b = 0.3\ \text{ms}^{-1}$ are constants adjusted by trial and errors in order for the model to fit the observed concentrations not only during the studied episodes but also over the five entire summer seasons of 1994 to 1998.

In the mixed layer the expressions of the mixing fluxes are:

$$F_m^+ = k(\overline{h})\frac{C_{\text{surf}}}{(\overline{h}-h_s)} + \frac{C_{\text{top}}}{(\overline{h}-h_s)}.\max\left(0, \frac{d\overline{h}}{dt}\right) \quad (1)$$

$$F_m^- = k(\overline{h})\frac{C_{\text{mix}}}{(\overline{h}-h_s)} + \frac{C_{\text{mix}}}{(\overline{h}-h_s)}.\max\left(0, \frac{d\overline{h}}{dt}\right) \quad (2)$$

The last term in equations (1) and (2) represents the entrainment of air from aloft, which is active only when $d\overline{h}/dt$ is positive, that is during the morning growth of the mixed layer.

2.2.3 Boundary conditions

Only five pollutants are advected from outside of the domain: Carbon monoxide, methane, ozone, peroxy acetyl nitrate (PAN) and formaldehyde. Thus only these have nonzero concentrations, which are taken to be equal both on the lateral side and at the top of the

model domain. The CO concentration at the boundary is taken as 100 ppb (direct sensitivity studies with other CO values have shown that this initial condition does not modify the modeled species concentrations), the methane concentration is taken as 1.8 ppm, and the other three have variable concentrations, taken as the "daily background values". In this study we first estimate the ozone background by the afternoon peak value of rural measurements taken on the upstream side of Paris, by the regional air quality network AIRPARIF, and second we estimate the PAN background value as 1/50 times the ozone value and the formaldehyde as 1/20 times the ozone value. These ratios are in agreement with episode values taken at rural sites in the Tropospheric Ozone Research (TOR) network [*Volz-Thomas et al.*, 1997]. These boundary conditions are only representative of vertically averaged values.

2.3 Chemistry

2.3.1 Gas phase chemistry

The gas phase chemical mechanism implemented in the model is the ModèlE Lagrangien de la CHImie de l'Ozone à l'échelle Régionale (MELCHIOR) mechanism [*Lattuati*, 1997] containing 70 species and more than 200 reactions. The mechanism is only discussed briefly here, as will be presented in more detail in a future paper (M. Beekmann and M. Lattuati, manuscript in preparation). The MELCHIOR mechanism can be regarded as an extended version of the European Monitoring and Evaluation Programme (EMEP) mechanism [*Simpson et al.*, 1993]. EMEP was recently compared to the much more extensive Institute För Vatten OCH Lüftvardsforskning (IVL) mechanism for an urban scenario (London plume) and showed very similar results. MELCHIOR was developed starting from an earlier mechanism of *Hov et al.*[1985].

The inorganic part of MELCHIOR is classical. As in the EMEP mechanism, the model hydrocarbons are representative for a class of hydrocarbons. The primary hydrocarbons included are methane, ethane, *n*-butane (representing alkanes with three or more C atoms), ethene, propene (representing internal and external alkenes with three or more C atoms), *o*-xylene (representing aromatic hydrocarbons), and isoprene (representing also terpenes). Again, as in the EMEP mechanism, the simplified degradation of these hydrocarbons yields 10 oxygenated species, including formaldehyde, acethaldehyde, methyl-ethyl-ketone, dicarbonyls, unsatured carbonyls, and alcohols.

In extension to the EMEP mechanism, the recombination reactions of peroxy radicals are treated in more detail, the number of reactions nevertheless being limited by only including self-reactions and reactions with CH_3O_2 and CH_3COO_2. Also, NO_3 is allowed to react with alkenes to form organic nitrates and to react with RO_2 radicals to form carbonyl compounds. Reaction rates were updated from *Atkinson et al.* [1997] and *De More et al.* [1997]. Heterogeneous reactions are not included, but the effect of clouds on the photolysis frequency is taken into account.

2.3.2 Radiation and deposition

The photolysis constants have a major influence in the ozone production and must be carefully evaluated. A "two-stream" radiative transfer model was used, as proposed by *Isaksen et al* [1977], and updated by *Jonson and Isaksen* [1991]. Note that the radiative model was used for meteorological conditions adapted to the cases studied (with an albedo of 0.13, a typical value for a site like the Paris area, and a temperature profile representative of midlatitude during summer). The photolytic constants used for the chemical mechanism

are the averaged values found from ground to 1000 m height. Clouds (with cloudiness C) may attenuate these values and are taken into account using very simple parameterizations (without a dependence on wavelength or zenith angle). The *Van Loon* [1994] formula is used with the multiplicative factor α to the constants, as $\alpha = 1 - 0.75.C^{3.4}$. Urban aerosols are not taken into account in this model version. Only dry deposition is taken into account (which is not a major problem, as the cases studied represent dry situations). The deposition velocities are considered as input parameters for the model, as a function of the model species and the simulated box.

2.4 Emissions

Hourly values of surface anthropic emissions are given for 15 primary pollutants: NO, NO_2, CO, SO_2, CH_4, and the 10 following nonmethane volatile organic compounds (NMVOC): ethane, *n*-butane, ethene, propene, *o*-xylene, formaldehyde, acetaldehyde, methyl ethyl ketone, methanol, and ethanol. As said before, these model species represent lumped categories of real NMVOCs. The whole procedure of model emissions construction follows two steps. We briefly recall here these two steps, and the reader is referred to *Vautard et al.* [1997] for further details. We used two data sources: the CITEPA (1993) inventory, providing annual totals of emissions of NO_x, SO_2, CO, CH_4, and NMVOCs (nonspeciated), and the Generation of European Emission Data for Episodes (GENEMIS) project [1994] database, used for NMVOC speciation and temporal disaggregation of annual totals to hourly values (Figure 2).

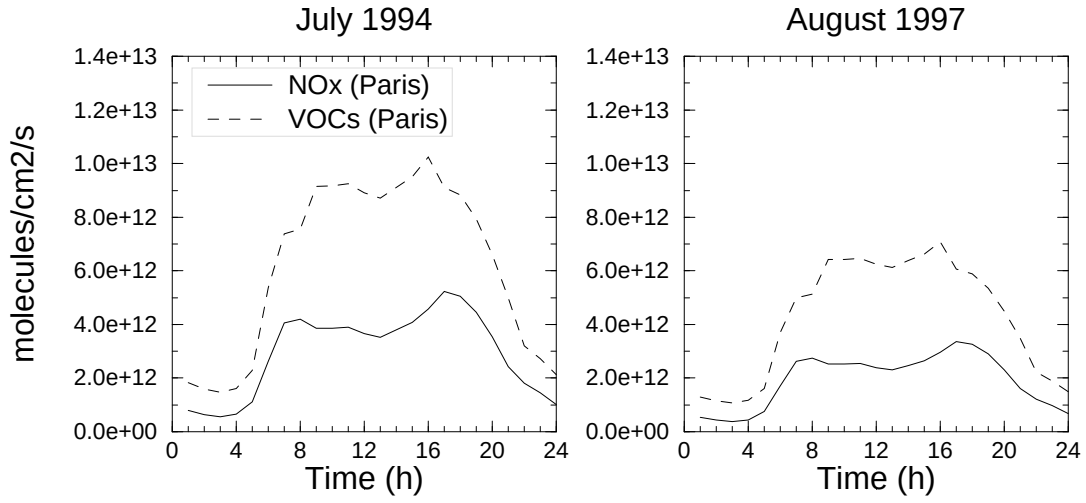

Figure 2: *Diurnal evolution (from 0 to 24h) of VOCs and NOx surface emissions (in molecules.cm^{-2}.s^{-1}) used for the studied cases of July 1994 and August 1997.*

The first step is speciation and temporal disaggregation of annual totals within each administrative disctrict: annual emissions of NO_x are first speciated as 5% of NO_2 and 95% of NO. Then we use the GENEMIS NMVOC speciation for the same districts and for six types of emission categories (traffic, solvents, industry (except solvents), energy extraction/production, residential (except solvents), and agriculture. For each activity, we then obtain a speciation, in terms of 32 NMVOC National Acid Precipitation Assessment Program (NAPAP) classes [*Middleton et al.*, 1990] for annual emissions. Temporal

variations are then calculated on the basis of GENEMIS data again, for three day types (weekday, Saturday, and Sunday), for each calendar month, each hour, and each activity sector. Only the weekday diurnal profile for traffic is not taken from the GENEMIS database, but from a recent publication of the emission profile of CO in the Paris area by *Sallès et al.* [1996].

Once the disaggregation step is performed, an aggregation step, for the lumping of NMVOCs into model species, is achieved using the *Middleton et al.* [1990] procedure using a time-integrated OH concentration (INTOH) of 1.0 ppt min as a control parameter value. We noticed that results are fairly insensitive to the value of INTOH. Isoprene is considered as the only primary biogenic pollutant. Its emission parameterization follows the model of *Guenther et al.* [1993]. Emissions of isoprene thus depend on temperature, while anthropic emissions do not (but probably should).

2.5 Numerics

Since physical and chemical processes are expressed in terms of fluxes, they can easily be integrated numerically all together, thus avoiding the classical "operator splitting" method which can lead to errors in certain circumstances [*Lanser and Verwer* 1998]. In fact, all model equations can be written under the following form:

$$\frac{dC_i(t)}{dt} = P_i(C_i(t),t) - L_i(C_i(t),t)C_i(t),$$

which allows the use of a variant of the classical quasi-stationary state approximation (QSSA) scheme. This variant simply consists of the implicit midpoint formula. A first iteration simply consists of the classical explicit QSSA formula:

$$\begin{aligned} C_i(t+\delta t) &= C_i^e(t) + (C_i(t) - C_i^e(t)) \\ &\quad \exp\left[-L_i(C_i(t),t)\delta t\right], \end{aligned}$$

where $C_i^e(t)$ corresponds to the equilibrium value as

$$C_i^e(t) = \frac{P_i(C_i(t),t)}{L_i(C_i(t),t)}.$$

The following iterations are performed as

$$\begin{aligned} C_i(t+\delta t) &= C_i^e(t+\delta t/2) + (C_i(t) - C_i^e(t+\delta t/2)) \\ &\quad \exp\left[-L_i(C_i(t+\delta t/2),t)\delta t\right], \end{aligned}$$

where the production and loss terms are estimated at the middle of the interval. This implicit version of QSSA provides a great stability to the original scheme and is efficient in terms of accuracy, since two iterations and a time step of 30 s were found to yield small errors relative to the same method using time steps of 1 s. This modified QSSA scheme was also compared to the TWOSTEP algorithm proposed by *Verwer and Simpson* [1995] and also yielded small differences.

2.6 The adjoint model formulation

As stated in the section 1, the main objective of an adjoint model is the calculation of the gradient $\nabla H(X)$ of a scalar function $H(X)$. This gradient depends on the prognostic variables of the model, here the pollutant concentrations, with respect either to initial

conditions or model parameters. The appendix describes how the adjoint of a model can indeed allow the calculation of such gradients.

In the case of this study, we use the adjoint model of CHIMERE for sensitivity calculations. Then, we aim at estimating the sensitivity of a simulated peak of a pollutant with respect to model parameters. For the results presented in the next sections, we define three types of scalar function $H(X)$: peak values of O_3, O_x (= O_3+NO_2), and NO_2 (hereafter called $[O_3]_{\max}$, $[O_x]_{\max}$ and $[NO_2]_{\max}$, respectively), on July 12, 1994 and August 12, 1997. Units used for sensitivities are percent by percent (%/%): For example, results for the sensitivity of $[O_3]_{\max}$ to the rate of the first chemical reaction (denoted by R_1), will be calculated as $(\partial[O_3]_{max}/\partial R_1)(R_1/[O_3]_{max})$. The results that will be given refer to changes in the parameters imposed during one hour.

The adjoint of the CHIMERE model has been developed on a line-by-line basis, reversing the order of operations and switching inputs and outputs of routines. Thus the gradients are calculated in an exact manner, to the computer accuracy (64 bits). The adjoint model was tested by the Taylor expansion verification method.

3 The two episodes under study: 12 July 1994 and 12 August 1997

In this paper the periods of the July 11 and 12, 1994 and the August 11 and 12, 1997 are chosen for the sensitivity study. This selection was made because (1) both periods correspond to strong photochemical pollution events over the Paris area, and (2) the origin of the events is apparently different, due to different local meteorological conditions. Both periods are different also from a chemical point of view, as we shall see below. From urban and rural O_3 and NO_2 measurements in and around the Paris region performed by the AIRPARIF air quality survey network, it appears that local O_x production was more intense during July 12, 1994 while the more homogeneous measurements on August 12, 1997 suggest larger scale ozone advection, (see Figure 3). In the following, the evolution of meteorological parameters is discussed in more detail.

3.1 Meteorological situations

The surface layer temperatures are values at the first ECMWF model level ($\approx$ 35 m) (see Figure 4). Maximum values are similar for August 11, 1997 ($T \approx 28^oC$ around 14h) and August 12, 1997 (T$\approx 30^oC$ around 1400 hours). On July 11 and 12, 1994, maximum values of respectively $T \approx 24^oC$ (1600) and $T \approx 29^oC$ (1500) are observed.

For the July 1994 period, the mean wind speed in the surface layer (Figure 4) appears to be rather constant, with $|U| \approx$ 2m s^{-1}. A decrease in wind speed values is oberved for the period of August 1997: While wind speed was rather constant on August 11, 1997, $|U| \approx 3m.s^{-1}$, one observes an important decrease during August 12, 1997, from $|U| \approx$ 3m s^{-1} to $|U| <$ 1m s^{-1} at the $[O_3]_{\max}$ time. This corresponds to a continuous increase of the residence time of pollutants in the central model box (30 km wide) during that day from approximately 3 hours for U=3 m s^{-1} to 8 hours for U=1 m s^{-1}.

For both periods the boundary layer height $\overline{h}$, as derived from ECMWF potential temperature profiles (see section 2.1.2) displays maximum values typical for sunny summer days. The maximum height is larger on July 11, 1994 (2150 m) than on August 11, 1997 (1400 m), and the maximum is reached earlier on July 12, 1994 (1300) than on August 12, 1997 (1400). Thus vertical mixing and dilution of emissions will be more important

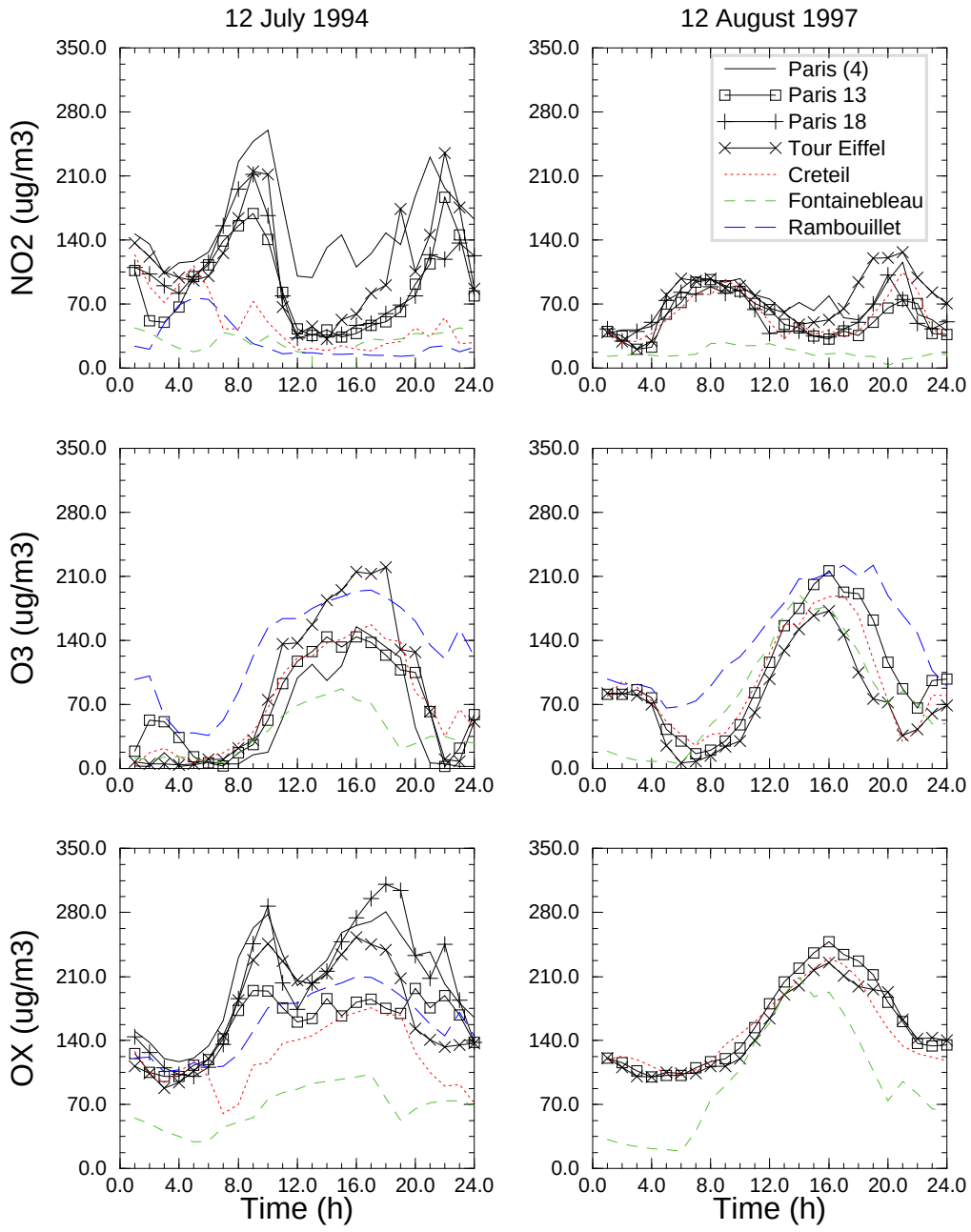

Figure 3: *Ground measurements of NO_2 (up), O_3 (middle) and O_x (down) for the two days studied: 12 July 1994 (left) and 12 August 1997 (right).*

on July 12, 1994.

3.2 Ground measurements of O_3 and NO_2

Figure 3 presents hourly average ground measurements of NO_2, O_3 and O_x over the model domain (data issued from the AIRPARIF network), on July 12, 1994 and August 12, 1997 (from 0000 to 2400 UT). On July 12, 1994, values together with the daily rural peaks of eastern rural stations suggest background ozone values of about 60 ppb, which were

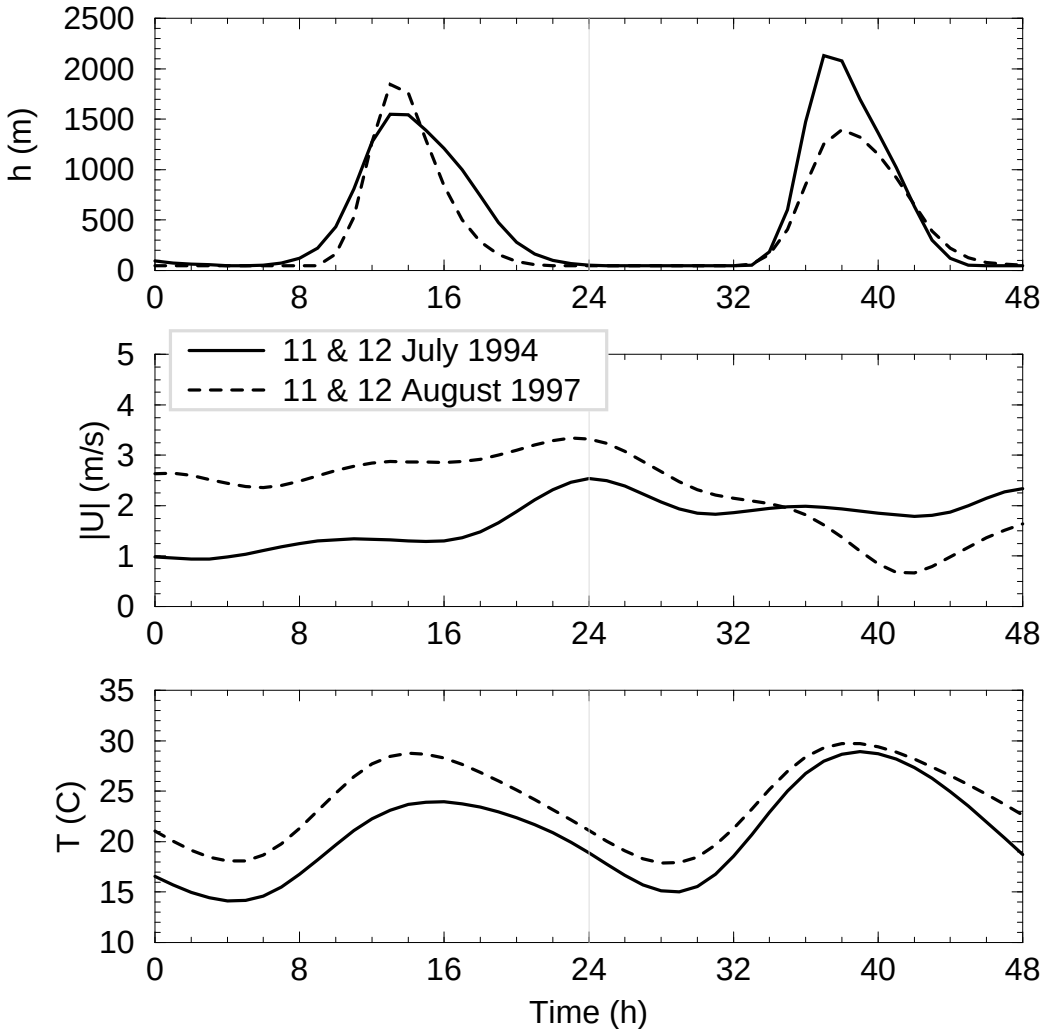

Figure 4: *Comparison of boundary layer height $\overline{h}$ estimated from ECMWF data (a), surface layer wind speed (in $m.s^{-1}$) (b) and surface layer temperature (in ^oC) (c) for both periods studied: 11, 12 July 1994 (solid line) and 11, 12 August 1997 (dashed line).*

taken as the model boundary conditions. It is noteworthy that all rural stations display much lower values than urban ones, indicating the strong photooxidant build up during this episode. A different behavior is observed on August 12, 1997. The spread of ozone concentrations is much less pronounced with rural values comparable to urban ones. We are led to conclude that at least a significant fraction of the ozone is advected into the domain, while local production seems less important than for July 12, 1994. In the case of August 12, 1997, 73 ppb of background ozone value was used in the model.

3.3 Comparison of model simulations with measurements

Figure 5 compares the diurnal variations of O_3, NO_2, and O_x concentrations, as simulated in the surface layer of the central model box and as averaged over all observations in this box. The NO_2 peak in the morning is very well reproduced on July 12, 1994, while somewhat overestimated on August 12, 1997. The afternoon ozone and O_x peaks on July

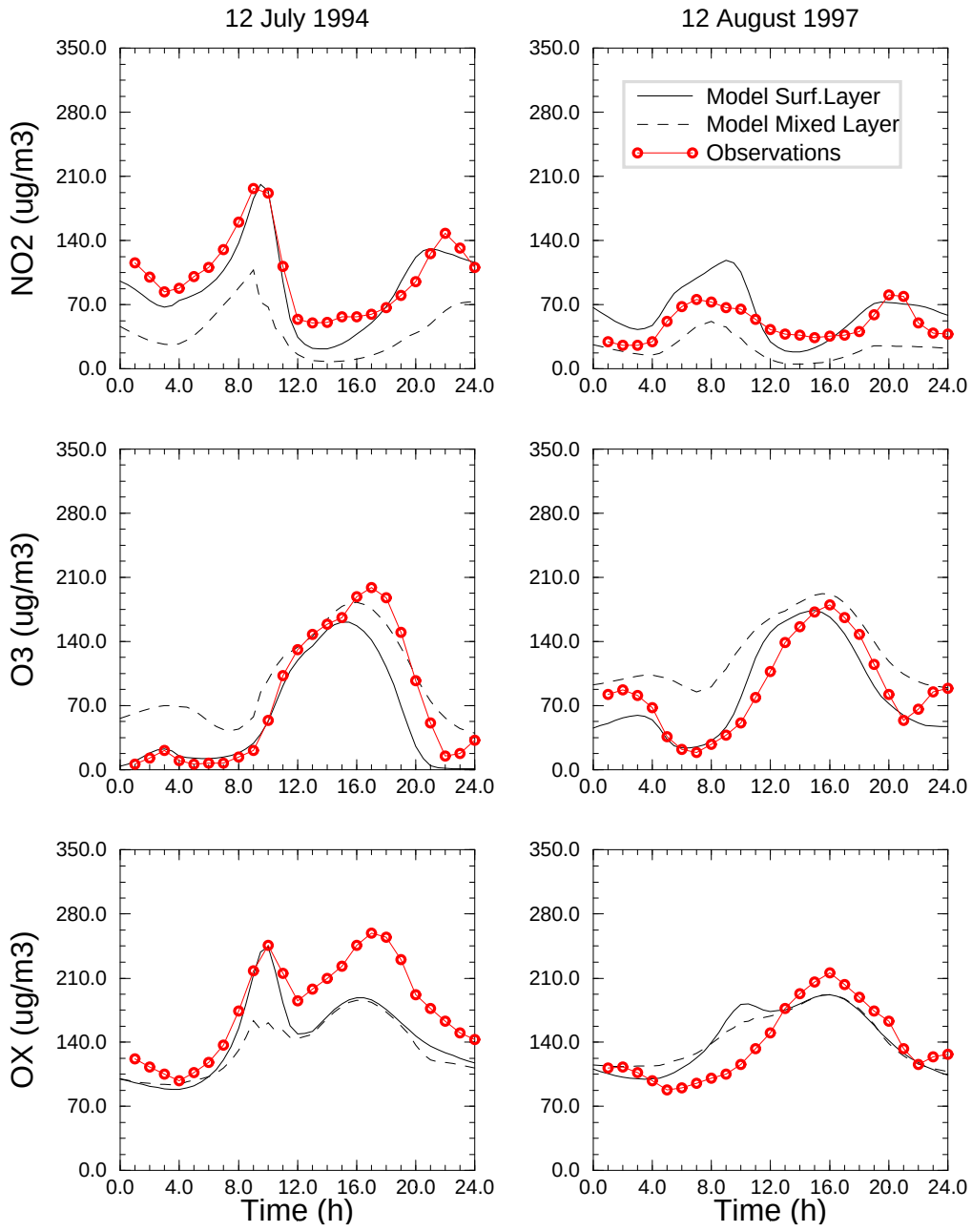

Figure 5: *Modelled values of NO_2, O_3 and O_x concentrations for the 12 July 1994 (left) and the 12 August 1997 (right). For both days, figures at top, middle and bottom represent the NO_2, O_3 and the O_x evolution from 0 to 24h, respectively. The solid line is the result for the surface layer, and the dashed line for the mixed layer. These values are comparable to the measurements, presented in the figure (3), and to the red line with circles corresponding to urban measurements averaged values.*

12, 1994 are underestimated by the model and appear 1-2 hours too early. However, one has to keep in mind the large spread in the urban measurements on that day which makes the comparison with the central model box corresponding to a 30 km average difficult. On the contrary, O_3 and O_x maximal concentrations are quite well simulated on August 12,

1997. In the following sections, sensitivity studies will be based only on model results and differences with observations should be kept in mind.

4 Sensitivity to emissions

4.1 Sensitivity to model species emissions

We first investigate the relative sensitivity of the photooxidant peaks to the model emitted species, and the time variations of this sensitivity. In the MELCHIOR mechanism, these species are NO, NO_2, CO, SO_2, CH_4, C_2H_6, n-C_4H_{10}, C_2H_4, C_3H_6, isoprene (C_5H_8), o-xylene (C_8H_{12}), HCHO, CH_3CHO, $CH_3COC_2H_5$, CH_3OH, and C_2H_5OH. As pointed out in section 2.4 each VOC species in the model represents in general a class of compounds. Besides, sensitivities are calculated by considering infinitesimal emission changes taken as uniform over all surface model boxes.

In Figure 6, we display for both July 12, 1994 and August 12, 1997 the sensitivity of the photooxidant peaks. In general, the most sensitive species is NO, followed by the most reactive VOCs: o-xylene, propene, ethene, and n-butane. It is interesting to notice that even in the case of the NO_2 peak, the sensitivity to NO_2 emissions is quite low. We also remark that, except for sensitivity of O_x to NO emissions, the sensitivity patterns are qualitatively similar during July 12, 1994 and August 12, 1997. We now examine separately each case. Note that as surface emission are considered, all the following results give sensitivities of surface layer pollutants to surface layer emissions.

4.1.1 Sensitivity of $[NO_2]_{max}$ to model emissions

The first important result revealed by Figures 6a and 6b is that an increase of any emitted species induces an $[NO_2]_{max}$ increase. The sensitivity to model emissions displays a peak just 1 hour or a few hours before $[NO_2]_{max}$, with NO sensitivity peaking later than VOC sensitivities, for the two days. At the sensitivity peak (0800), a change of 1% of NO emission at the peak results in a change of 0.21% the $[NO_2]_{max}$ value on August 12, 1997, and of 0.1% on July 12, 1994. VOC sensitivity peaks earlier (by about 1 hour) since NO_2 formation through VOC emissions essentially results from the net radical cycle, which can be formally written as:

$$VOC + OH \rightarrow 2.NO_2 - 2.NO + OH + CARB$$

where CARB represents carbonyl compounds. This transformation is slow, especially during morning hours when [OH] is weak, with a timescale of a few hours for the most reactive VOCs, hence the delay in sensitivity relative to NO emissions. Second, we remark that NO sensitivity is about twice as large on August 12, 1997 than on July 12, 1994, while VOC sensitivities are twice as low. This could be a hint of a qualitative difference in chemical regimes between the two days, as will be further discussed in section 4.1.3.

4.1.2 Sensitivity of $[O_3]_{max}$ to model emissions

These results are displayed in Figures 6c and 6d. All sensitivities are positive, except for NO and NO_2 (with a very small sensitivity for the latter). The maximum of VOC sensitivities occurs during the morning, 4-6 hours before $[O_3]_{max}$: This illustrates the fact that ozone production by VOC oxidation is a slow process. For o-xylene and propene an increase of 1% in the emissions induces an increase of $[O_3]_{max}$ of 0.02% on July 12, 1994

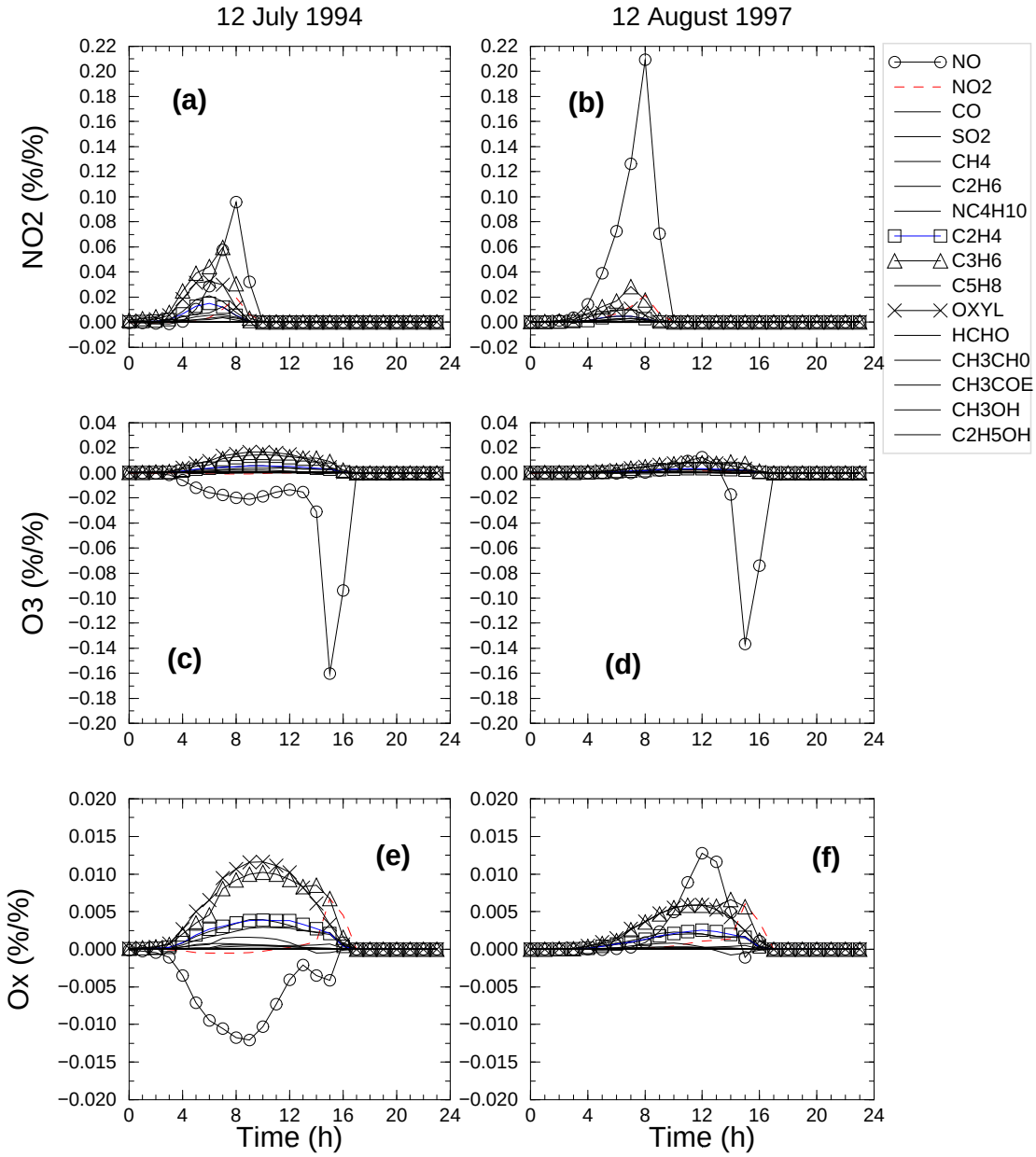

Figure 6: *Sensitivity (in %/%) of* $[NO_2]_{max}$ *(a,b),* $[O_3]_{max}$ *(c,d) and* $[O_x]_{max}$ *(e,f) to the emitted model species. Results are expressed on left side for the 12 July 1994, and right side for the 12 August 1997.*

and 0.01% on August 12, 1997 at the time of the sensitivity peak at 1200. This illustrates the fact that among VOC emissions, mainly aromatic and olefin compounds contribute to ozone build up in an urban environment.

The large negative sensitivity peak for NO occurs during the hour preceding $[O_3]_{max}$, due to the fast titration of ozone by NO. It is interesting to notice that on July 12, 1994, a second negative peak is observed in the NO sensitivity curve at 0900, while the

correponding peak on August 12, 1997 is positive and peaks near 1100. This important difference can be explained by a difference in chemical regimes between the two days as will be discussed later.

4.1.3 Sensitivity of $[O_x]_{max}$ to model emissions

The advantage of the O_x formulation is the release of photochemical equilibrium effect in the photooxidant budget. This is clearly seen in Figures 6e and 6f. The sensitivities to NO_x behave similarly to those for $[O_3]_{max}$, but the large negative afternoon peak is removed. The sensitivity to NO_x is always negative during July 12, 1994, but positive during almost all of August 12, 1997. We conclude that there is a clear difference in the chemical regime between July 12, 1994 and August 12, 1997. Also, sensitivity to VOC emissions is twice as large on July 12, 1994 as on August 12, 1997. Another interesting feature revealed by O_x analysis is that the afternoon O_x peak is essentially sensitive to morning emissions in both cases. As said before, this illustrates the timescale of photochemical oxidant build up at least of the order of several hours. The increase of sensitivity with decreasing time of the day is limited by two factors: (1) emissions become lower during early morning hours and during the night, and (2) ozone produced from these emissions will be increasingly advected out of the model domain and cannot contribute significantly to the peak values.

4.1.4 Chemical regime difference

In this section we give an explanation of the different sensitivities towards emission changes presented up to now. Several studies [e.g., *Sillman et al.* 1990; 1999] indicate that photooxidant production can be more sensitive either to NO_x emissions (NO_x-limited regimes) or to VOC emissions (VOC-limited regimes).

A major difference between these regimes is the relative strength of the two radical sink paths:

$$NO_2 + OH + M \rightarrow HNO_3 + M \tag{3}$$

or

$$\begin{cases} RO_2 + HO_2 \rightarrow \text{peroxyde} & \text{(a)} \\ RO_2 + RO_2 \rightarrow \text{peroxyde} & \text{(b)} \\ HO_2 + HO_2 \rightarrow H_2O_2 + O_2 & \text{(c)} \end{cases} \tag{4}$$

where the reaction (3) is dominant in a VOC-limited regime, and the system (4a)-(4c) is dominant in a NO_x-limited regime. As Figure 7 shows, the major radical loss path on July 12, 1994 is reaction (3); thus the regime is VOC-limited and consequently the sensitivity of photooxidant production is positive with respect to VOC emissions and negative with respect to NO_x emissions. In contrast, on August 12, 1997, both RO_2 and HO_2 recombination reactions play a significant role, especially during the afternoon. Consequently, the chemical regime is NO_x-limited, the sensitivity to NO_x emissions is positive. In fact, the sensitivity to VOC emissions is also positive, but to a lesser extent than on July 12, 1994.

The difference in chemical regimes between both days becomes even more evident in Figure 8 where the O_x concentrations (weighted and averaged over the two model layers) at 1600 are plotted as a function of the NO_x and the VOC emissions. For each situation under study, we have performed a series of simulations, by keeping all the meteorological and boundary parameters unchanged and varying only the NO_x and the VOC emissions which are weighted by a pair of coefficients (E_{NO_x},E_{VOC}) ranging between 0 and 2.

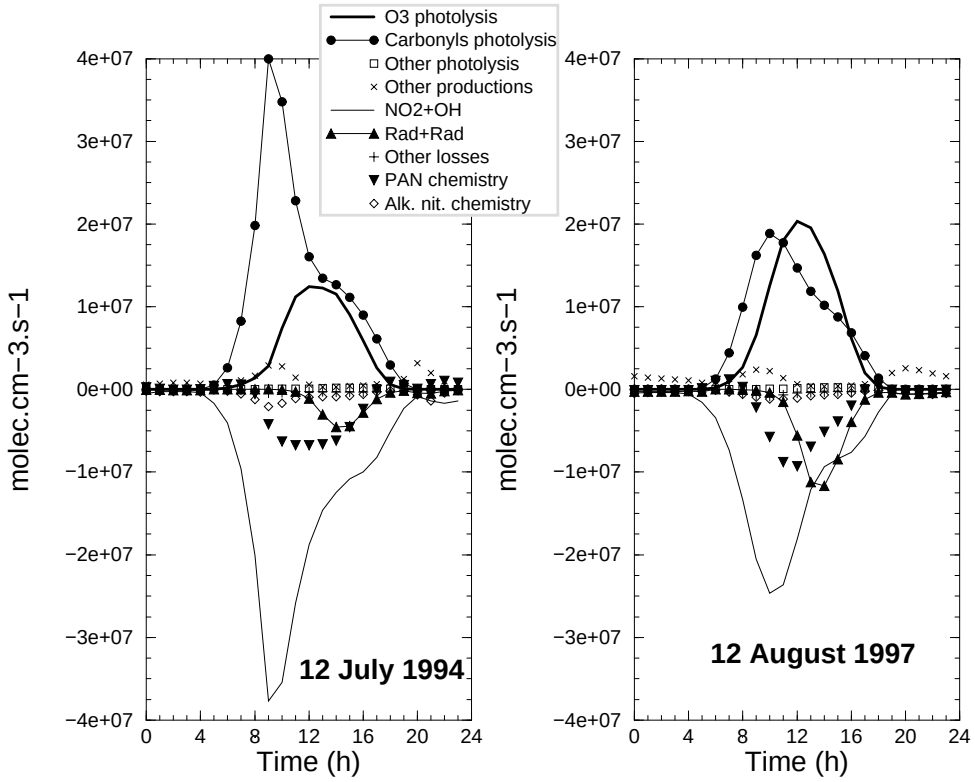

Figure 7: *Radical budget for each day (in molecules/cm^3/s for both figures) weighted and averaged over the two model layers (surface and mixed layer of the Paris box). The 'Rad+Rad' term gathers all radicals recombination reactions and 'Alk. nit.' stands for 'Alkyl nitrates'.*

In this Figure, one clearly identifies the two chemical regimes described previously. In both situations, there is a transition curve defined by

$$\frac{\partial[O_x]}{\partial \mathrm{E_{NO_x}}}(\mathrm{E_{NO_x}}, \mathrm{E_{VOC}}) = 0$$

or

$$\mathrm{E_{VOC}} = \Psi(\mathrm{E_{NO_x}})$$

This curve is approximately a straight line and delimits two regions of distinct sensivitivy. For $E_{\mathrm{VOC}} \leq \Psi(E_{\mathrm{NO_x}})$, the system is thus VOC/NO_x sensitive, whereas for $E_{\mathrm{VOC}} \geq \Psi(E_{\mathrm{NO_x}})$, the system is NO_x sensitive.

It clearly appears from Figure 8 that on July 12, 1994, the Parisian boundary layer lies in the VOC/NO_x sensitive region (the point (1,1) is located on the right side of the transition line) whereas on August 12, 1997, it lies in the NO_x-sensitive region. However, in both cases, it is not very far from the transition line, so that on the August 12, 1997, the chemistry is not only NO_x sensitive but also to a lesser extent VOC sensitive. Moreover, in both cases, a change in the NO_x and VOC emissions strength could result in a change in the state of the system. Thus an error in the emissions database could have caused a misidentification of the chemical regime for one or both days. Another difference in the isopleths for both days is that isolines are closer and thus gradients larger, both with respect to NO_x as to VOC emissions, on July 12, 1994 than August 12, 1997. This also

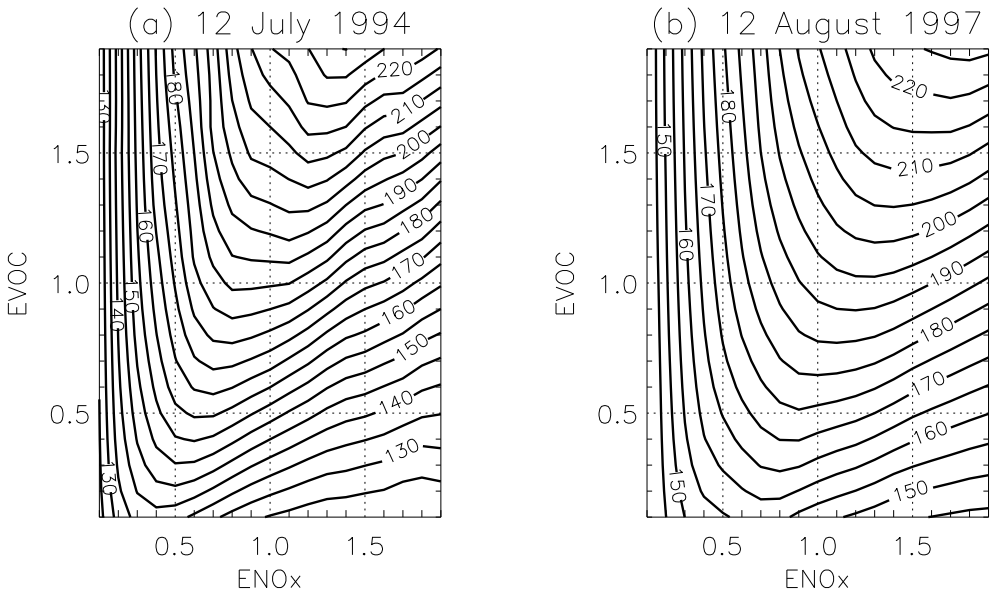

Figure 8: *O_x concentration (in $\mu g.m^{-3}$) at 16 h, weighted and averaged over the two model layers, as a function of the NO_x and the VOC emissions weight (respectively E_{NO_x} and E_{VOC}). Results are expressed for the 12 July 1994 (left) and 12 August 1997 (right).*

corresponds to the larger local photochemical ozone production on the former day, as noted before.

The origin of distinct sensitivity regimes for the two days studied has to be searched for in the meteorological parameters and emissions strengths. First, as shown in Figure 2, the VOC and NO_x anthropic emissions are larger on July 12, 1994 than on August 12, 1997. Indeed, as can be seen in Figure 8, an equal increase in both VOC and NO_x makes a chemical regime more VOC limited. Second, the relative and absolute contribution of ozone photolysis to the radical budget is larger on August 12, 1997 (Figure 7), linked to a larger content of water vapor over the Paris region, favoring the formation of OH radicals from O(1D) (Table 1). This increase in radical production shifts the chemical system more towards a NO_x limited regime [e.g., *Kleinman*, 1994]. Third, it has been shown [*Honoré et al.*, 1998] in idealized cases that the wind speed is a key parameter controlling the sensitivity state of an urban atmosphere: As it decreases, the system shifts from the VOC-sensitive region towards a NO_x-sensitive one. An explanation for this shift is that the lifetime of NO_x relative to OH is lower than that of the average VOCs. Hence, the longer the residence time of the air mass in an urban agglomeration is, the more VOC will accumulate with respect to NO_x and the chemical regime be shifted from VOC limited to NO_x limited. Actually, for the days studied here, the afternoon wind speed is almost twice as low on the August 12, 1997 than on the July 12, 1994. All three reasons point towards the same direction of a more NO_x limited regime on August 12, 1997. However, it is beyond the scope of this paper to quantify each of these causes.

4.2 Sensitivity of photooxidant peaks to emissions by activity categories

Reducing emissions pollutant by pollutant is evidently not possible from the practical point of view. Therefore we examine here the sensitivity of photooxidants with respect

Date and Time		12J94		12A97	
		9h	16h	9h	16h
Parameters	(unit)				
$[NO_2]$	(μ.g.m^{-3})	200.	40.	118.	32.
$[O_3]$	(μ.g.m^{-3})	30.	162.	44.	173.
$[O_x]$	(μ.g.m^{-3})	220.	188.	158.	190.
Temperature	(^{o}C)	20.	28.	23.	29.
Wind speed	(m.s^{-1})	1.8	1.9	2.	1.1
$\overline{h}$	(m)	50.	1900.	50.	1330.
q	(g/kg)	13.2	13.3	21.2	20.7

Table 1: *Values of the pollutants peaks chosen for the sensitivity study. One also reports the values of the meteorological parameters at the same time, issued from the ECMWF analysis, and estimated in the surface layer.*

to emissions in activity categories. In the present study, emissions are grouped into six categories: TRAF for traffic, RESI for domestic and small business activities, SOLV for solvents, INDU for industry (other than solvents), ENER for power production and AGRI for agriculture. Traffic emissions are the dominant source of both NO_x and VOC emissions, the solvent/industry sector is unique as it exclusively consists of VOC emissions. As in the previous section, we plot in Figure 9 the hourly-distributed sensitivity of photooxidant peaks to surface layer emissions per categories on July 12, 1994 and August 12, 1997.

4.2.1 Sensitivity of $[NO_2]_{max}$

For both days studied, the sensitivity of $[NO_2]_{max}$ to emissions by activity category is positive, meaning that a reduction of emissions would always lead to a $[NO_2]_{max}$ concentration decrease. Not surprisingly, by far the most sensitive category is traffic. A reduction of 1% of the traffic emissions at sensitivity peak (near 0700) leads to a reduction of 0.15% of the NO_2 peak on July 12, 1994, and 0.2% on August 12, 1997. The second most sensitive category is solvents. Traffic sensitivity is more pronounced on August 12, 1997, while solvent sensitivity is more pronounced on July 12, 1994. This is in line with sensitivities found with respect to individual pollutants (Figure 6) and points again to differences in the chemical regime between both days. Finally, we remark that the other emission categories (especially ENER) have only a poor contribution to a $[NO_2]_{max}$ increase.

4.2.2 Sensitivity of $[O_3]_{max}$ and $[O_x]_{max}$

As for $[NO_2]_{max}$, $[O_3]_{max}$ is essentially sensitive to traffic and solvent emissions. During morning hours, $[O_3]_{max}$ is positively sensitive to traffic emissions, while it is negatively sensitive during afternoon hours before the ozone peak. On a timescale of several hours, traffic emissions act on photooxidant build up and on the timescale of several minutes, traffic NO emissions titrate ozone. The latter process evidently causes the negative afternoon peak which, by the way, disappears when looking at the O_x maximum. On July 12, 1994, the sensitivity for the solvent sector (with only VOC emissions) is stronger than or equal to the sensitivity of the traffic sector emissions, respectively for the O_3 maximum and for the O_x maximum. In contrast, on August 12, 1997, traffic emission reductions are always more effective in reducing O_3 and O_x peaks. This again illustrates that an optimal

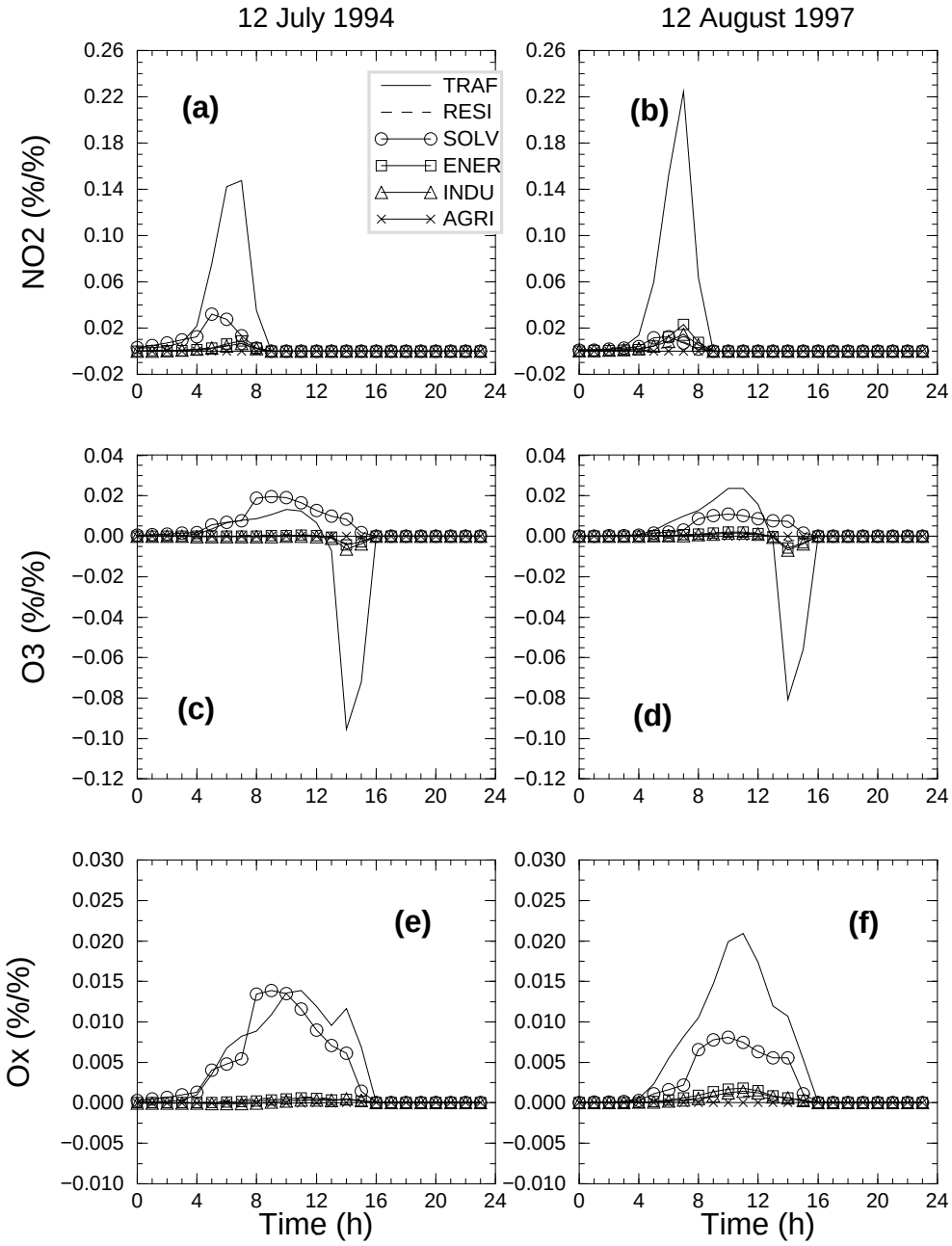

Figure 9: *Sensitivity (in %/%) of* $[NO_2]_{max}$ *(a,b),* $[O_3]_{max}$ *(c,d) and* $[O_x]_{max}$ *(e,f) to the emissions by activity sectors. Results are expressed on left side for the 12 July 1994, and right side for the 12 August 1997.*

emission reduction strategy has to take into account differences in the chemical regimes for individual days.

5 Sensitivity to reactions rates

Sensitivities of NO_2, O_3, and O_x peaks are examined as a function of each reaction rate coefficient. While we consider the pollutant peak in the surface layer, sensitivity is cumu-

Reaction	NO_2		O_3		O_x	
	12J94	12A97	12J94	12A97	12J94	12A97
Inorganic chemistry						
O_3+NO → NO_2	0.0372	0.1747	-0.3648	-0.2901	-0.2299	-0.1946
NO+HO2 → OH+NO2	0.0031	0.0033	0.1045	0.1124	0.0706	0.0786
NO_2+OH → HNO_3	-0.3169	-0.1521	-0.2688	-0.1670	-0.2088	-0.1385
NO + OH → HONO	-0.1233	-0.0251	-0.0104	-0.0031	-0.0071	-0.0022
COV attacks by OH						
C_3H_6+OH+M → $CH_3CH(O_2)CH_2OH$	0.1698	0.0671	0.0388	0.0214	0.0285	0.0169
o-xylene+OH → *o*-xylene(OH)O_2	0.1204	0.0399	0.0743	0.0294	0.0520	0.0219
Carbonyls compounds attacks by OH						
HCHO + OH → CO + HO_2	-0.0015	0.0021	-0.0194	-0.0003	-0.0089	0.0031
CH_3CHO+OH → CH_3CO_3	0.0178	0.0019	0.0093	0.0034	0.0071	0.0025
MGLYOX + OH → CH_3CO_3 + CO	-0.0015	-0.0009	-0.0241	-0.0092	-0.0147	-0.0055
Organic radicals conversion						
CH_3CO_3+NO → CH_3O_2+NO_2+CO_2	0.0529	0.0378	0.1522	0.1138	0.1161	0.0920
Organic nitrats and PAN						
CH_3CO_3+NO_2+M → PAN	-0.0528	-0.0378	-0.1498	-0.1121	-0.1148	-0.0912
PAN + M → CH_3CO_3+NO_2	0.0522	0.0383	0.1261	0.0985	0.0971	0.0802
Photolytic reactions						
O_3→2.OH	0.0225	0.0199	0.1303	0.0384	0.0770	0.0150
NO_2 → NO+O_3	-0.0665	-0.1758	0.3787	0.3294	0.2477	0.2271
HCHO → CO+2*HO_2	0.2530	0.0739	0.1351	0.0447	0.0881	0.0296
HCHO → CO+H_2	-0.0299	-0.0078	-0.0342	-0.0134	-0.0235	-0.0098
MGLYOX → CH_3CO_3+HO_2+CO	0.0657	0.0169	0.0582	0.0190	0.0376	0.0122
HONO → NO + OH	0.0905	0.0181	0.0079	0.0020	0.0053	0.0015

Table 2: *Relative sensitivity (%/%) of NO_2 (9h), O_3 (16h), O_x (16h) peaks values calculated in the urban surface layer to reaction rates coefficients integrated in all boxes and during all the day.*

lated in the two model layers for the urban box, so that results are representative for the whole boundary layer photochemistry. These sensitivities are calculated for all chemical reactions (%/%), again for changes of a reaction rate occuring during one hour. We first remark that the most sensitive reactions are generally the same for $[O_3]_{max}$ and $[O_x]_{max}$, but may be different for $[NO_2]_{max}$. It also becomes clear that only about 20 reactions are really sensitive. This strongly points towards the possibility of using drastically reduced chemical mechanisms for urban air quality modeling.

The family grouping shows that the highest sensitivities are obtained for (1) the inorganic chemistry, (2) photolysis reactions, (3) VOC oxidation by OH, (4) PAN chemistry, and (5) organic radical conversion. In order to select the most sensitive reactions, they are ranked as a function of the maximal value occuring during the day for NO_2, O_3 and O_X. Values are reported in Table 2.

Comparing both days studied, almost all reactions displayed, and in particular photolysis reactions, exhibit a higher sensitivity on July 12, 1994 than on August 12, 1997. The reasons for this behavior are again the difference in the chemical regime for the two days and the stronger local photochemical oxidant build-up on July 12, 1994. This day, the photooxidant production is limited by the presence of radicals; hence radical source reactions such as photolysis reactions become more sensitive.

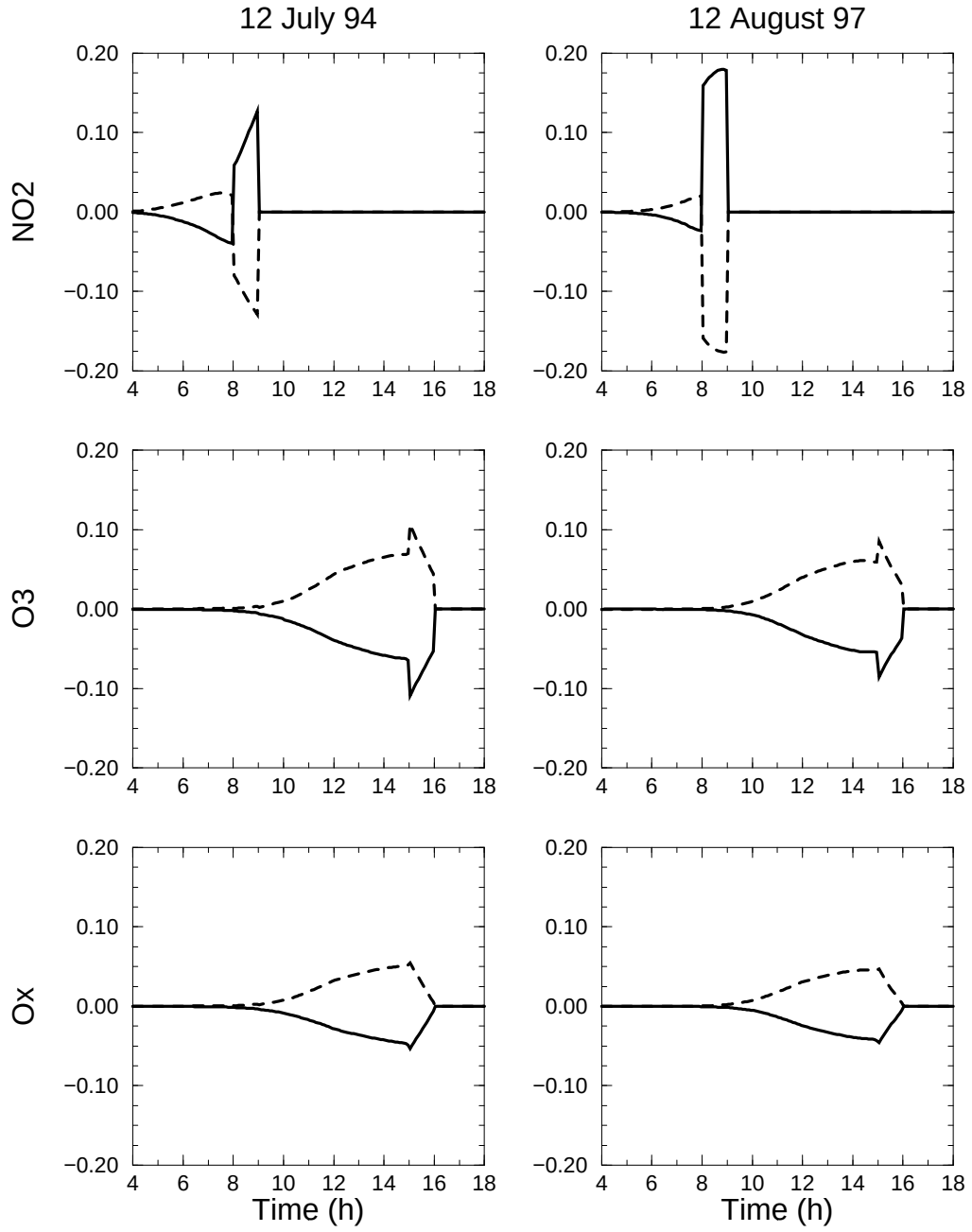

Figure 10: *Sensitivity of* $[NO_2]_{max}$, $[O_3]_{max}$ *and* $[O_x]_{max}$ *to the photochemical equilibrium: the black lines represent the reaction 'O_3+$NO \rightarrow NO_2$', and the dashed lines the reaction '$NO_2 \rightarrow NO$+O_3'. Figures at the left and at the right are for the 12 July 1994 and the 12 August 1994, respectively. Figures are the sensitivity of* $[NO_2]_{max}$, $[O_3]_{max}$ *and* $[O_x]_{max}$ *at the top, the middle and the bottom, respectively*

5.1 Sensitivity to photostationary equilibrium

We now turn to the time-distributed sensitivity of several important reactions reported in the previous tables. We display, in Figure 10, the time distribution of sensitivity to

the reaction rates coefficients of the reactions involved in the NO-NO_2-O_3 equilibrium, synthesized as

$$\begin{cases} NO + O_3 & \rightarrow & NO_2 & \text{Inorganic chemistry} & \text{(a)} \\ NO_2 & \rightarrow & NO + O_3 & \text{Photolysis} & \text{(b)} \end{cases} \quad (5)$$

Both reactions have an inverse effect, which is illustrated by the symmetric shape, but opposite sign for both sensitivity curves. During daytime, the reactions are fast, so one expects sensitivity to be highest just before peak time. Interestingly, the sensitivities of the NO_2 peak exhibits a change of sign, for both cases, one hour before the peak. During the hour preceding the peak, NO_2 formation via titration of NO emissions by ozone has a positive effect on the NO_2 peak while the opposite occurs a few hours before. This delayed negative effect reflects the additional radical sink (with subsequent decrease in O_x production) if an increased fraction of NO_x is present as NO_2.

By contrast, NO_2 formation by combination of NO and ozone always has a negative effect on the afternoon ozone and O_x peaks, with a maximum sensitivity near the peak time. The explanation is straightforward for the sensitivity of the ozone peak since this reaction acts as titration. For the sensitivity of the O_x peak, sensitivities have the same sign but lower amplitudes. Again, this is caused by the effect of a redistribution of NO_x species on the radical budget.

5.2 Sensitivity to VOC oxidation by OH

In order to illustrate the sensitivity to this group of reactions, we display the time-distributed results for two of them in Figure (11):

$$\begin{cases} C_3H_6 + OH + M & \rightarrow & CH_3CH(O_2)CH_2OH & \text{(a)} \\ CH_3CHO + OH & \rightarrow & CH_3CO_3 & \text{(b)} \end{cases} \quad (6)$$

First, we remark that sensitivities are positive for reaction 6(a) and negative for 6(b), before the peaks time. The positive sensitivity of $[NO_2]_{max}$, $[O_x]_{max}$ and $[O_3]_{max}$ to 6(a) is directly connected to the radical cycles linked to hydrocarbon oxidation: If the reaction rate coefficient increases, more OH can be transformed into HO_2 and RO_2 radicals which will react with NO and increase the O_x production. This extra O_x production is revealed by the increase of the NO_2 peak in the morning and by the ozone peak during the afternoon.

The sensitivity to the rate of reaction 6(b) is very interesting to study as it becomes negative only after about 14h. This can be explained by the competition between two processes: the acetyl peroxy radical, product of reaction 6(b), can either react with NO which subsequently forms one to two molecules O_x, or react with NO_2 to form PAN, with a loss of one radical and one molecule O_x. The distribution between both pathways displays a strong diurnal variation as a function of the NO / NO_2 ratio, peaking at noon, which explains the diurnal variation of the sensitivity.

5.3 Sensitivity to NO-to-NO_2 conversion

In order to investigate the effect of this group of reactions on photooxidant peaks, we display two examples in Figure (12) corresponding to reactions:

$$\begin{cases} NO + HO_2 & \rightarrow & OH + NO_2 & \text{(a)} \\ CH_3CO_3 + NO & \rightarrow & CH_3O_2 + NO_2 + CO_2 & \text{(b)} \end{cases} \quad (7)$$

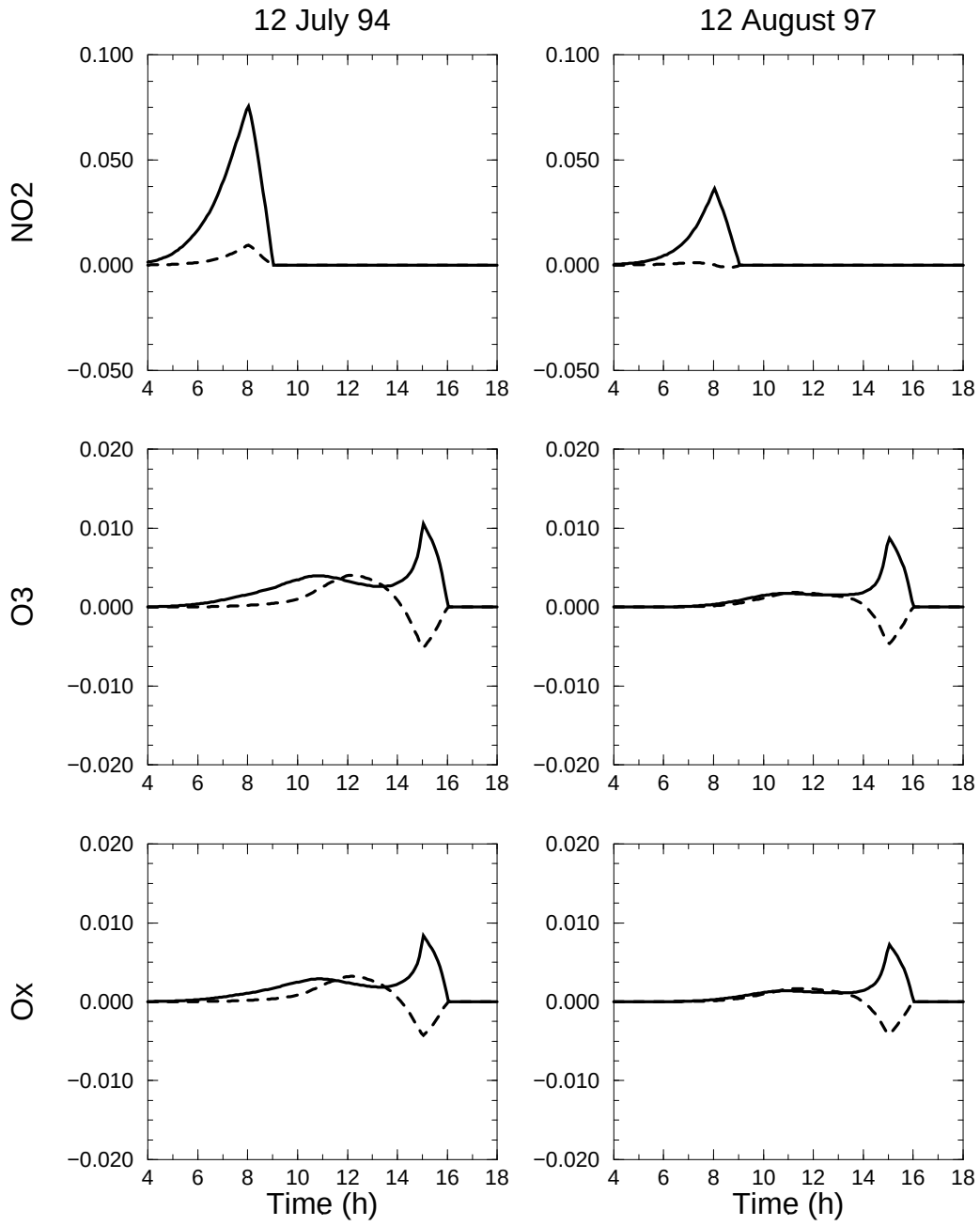

Figure 11: Sensitivity of $[NO_2]_{max}$, $[O_3]_{max}$ and $[NO_2]_{max}$ to the "VOCs and carbonyls compounds attacks by OH radicals reactions": The solid lines represent the reaction "C_3H_6+OH+M $\rightarrow$ $CH_3CH(O_2)CH_2OH$" and the dashed lines the reaction "CH_3CHO + OH $\rightarrow$ CH_3CO_3". Plots are arranged as in Figure 10

Both reactions display a positive sensitivity almost all day long, as NO to NO_2 conversion directly corresponds to O_x production. The second reaction is more sensitive especially for the NO_x peak and also for the O_3 and O_x peak one hour before. This is again explained by the fact that this reaction is competing with PAN formation, while reaction 7(a) is anyway the dominant pathway.

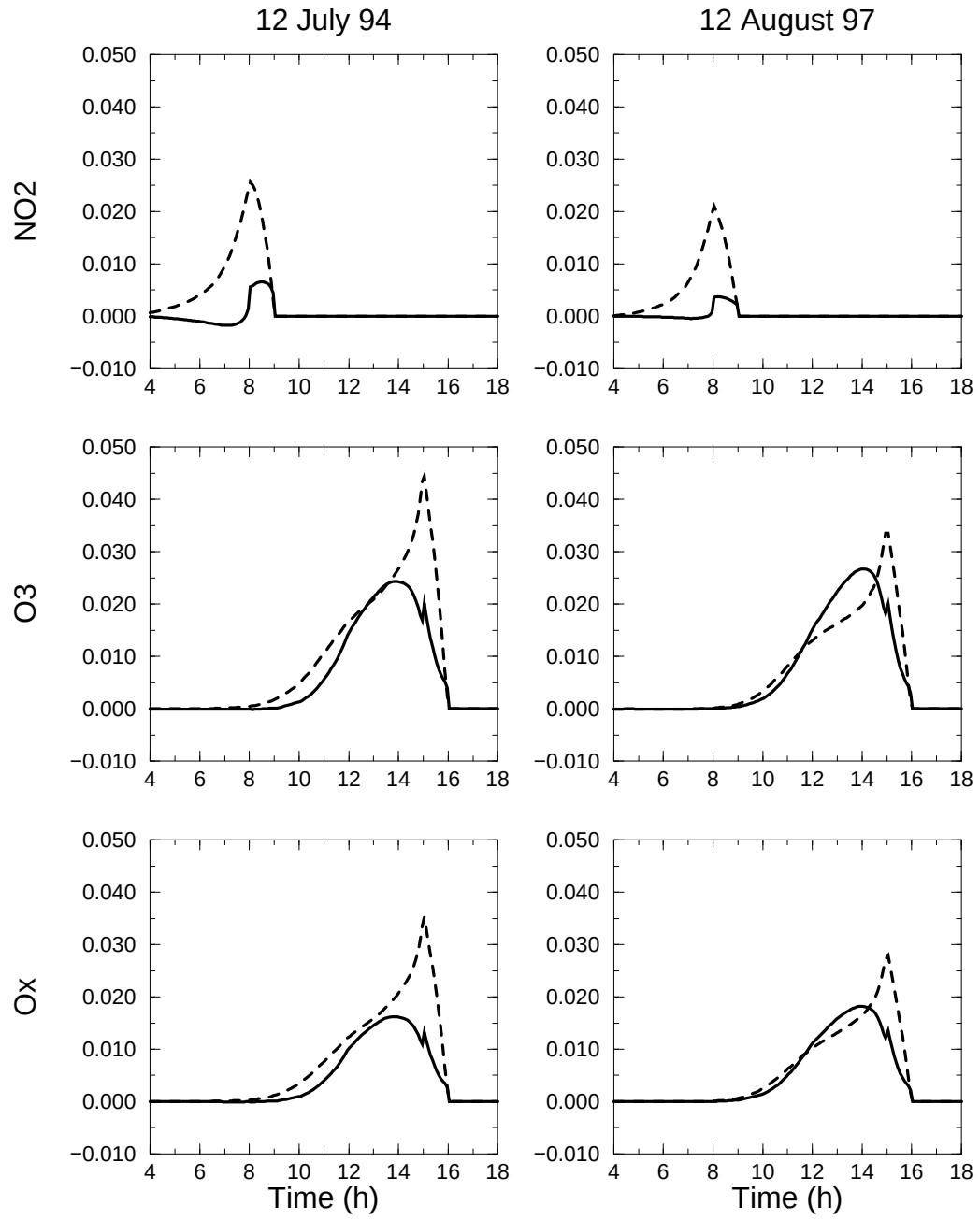

Figure 12: *Sensitivity of* $[NO_2]_{max}$, $[O_3]_{max}$ *and* $[O_x]_{max}$ *to the conversion of NO into* NO_2*: The black lines represent the reaction '*$NO+HO_2 \rightarrow OH+NO_2$*' and the dashed line the reaction '*$CH_3CO_3+NO \rightarrow CH_3O_2+NO_2+CO_2$*'. Figures are presented as for the figure (10)*

Looking at the differences between both days, one notes that sensitivities with respect to the NO_2 peak are again higher during July 12, 1994 than during August 12, 1997. Again, it appears that the NO_2 peak is much more due to photochemical O_x production on July 12, 1994 while for the August 12, 1997 simple mixing with residual layer ozone

and conversion into NO_2 strongly dominates the peak concentration. This also has to correspond to stronger pollutant concentrations in the early morning of July 12, 1994 which are indeed observed by the AIRPARIF network: The NO peak occurs between 0700 and 0800 for both days, with maximum values of 186 and 47 μ g m^{-3} for July 12, 1994 and August 12, 1997, respectively.

5.4 Sensitivity to photolysis reactions

Sensitivities of photooxidant peaks to some photolysis reactions are displayed In Figures (13), (14). We first examine the sensitivity to ozone, methyl-glyoxal (MGLYOX) and formaldhyde photolysis:

$$\begin{cases} O_3 & \rightarrow & 2\ OH & \text{(a)} \\ MGLYOX & \rightarrow & CH_3CO_3 + HO_2 + CO & \text{(b)} \end{cases} \quad (8)$$

$$\begin{cases} HCHO & \rightarrow & CO + 2.HO_2 & \text{(a)} \\ HCHO & \rightarrow & CO + H_2 & \text{(b)} \end{cases} \quad (9)$$

For all photolysis reactions creating radicals (reactions (8a), (8b) and (9a)) an increase of the reaction rates coefficients results in an increase of O_x values on July 12, 1994. However, the time distribution of sensitivities is different, as well as the relative behavior for the two days studied. For the sensitivity of the NO_2 peak, we remark that ozone photolysis is not important, whereas methyl-glyoxal and formaldehyde photolysis is sensitive. This is in agreement with the contribution of the photolysis of different species to the radical budget displayed in Figure 7. Indeed, ozone photolysis, creating O(1D) radicals, occurs in the UV and becomes important only around noon. As already seen for other reactions, carbonyl photolysis is also more sensitive for the NO_2 peak on July 12, 1994 than on August 12, 1997, due to the greater photochemical activity on the morning of July 12, 1994.

Concerning the afternoon O_3 and O_x peaks, photolysis of HCHO $\rightarrow$ CO + 2HO_2 is again much more sensitive on July 12, 1994 than on August 12, 1997, because of the VOC-or-radical-limited chemical regime on July 12, 1994. Surprisingly, during morning hours, ozone photolysis even has a slightly negative sensitivity on August 12, 1997 for the O_3 and O_x peaks. Probably, the ozone molecule initially lost is not recovered by extra O_x production through the created OH radicals.

Finally, the sensitivity of the non radical forming pathway of formaldehyde photolysis is always slightly negative, as it competes with the radical forming photolysis pathway (Figure (14)).

5.5 Sensitivity and uncertainties

In order to obtain the local uncertainty of modeled photooxidant production with respect to reaction rate coefficients, the above determined sensitivities have to be combined with the individual uncertainties of reaction or photolysis rates. Indeed, if the relative accuracy of a chemical reaction rate coefficient is x% and the relative sensitivity of O_x peak is y%/%, one would expect each independant reaction induces an overall error of xy% on the peak value. This reasoning is correct only if the sensitivities are linear, which means that the perturbation caused by an infinitesimal change in a rate constant can be extrapolated to the actual uncertainties. For each reaction studied in this paper, several authors have previously given an uncertainty value. Considering each reaction, one by one, it is possible

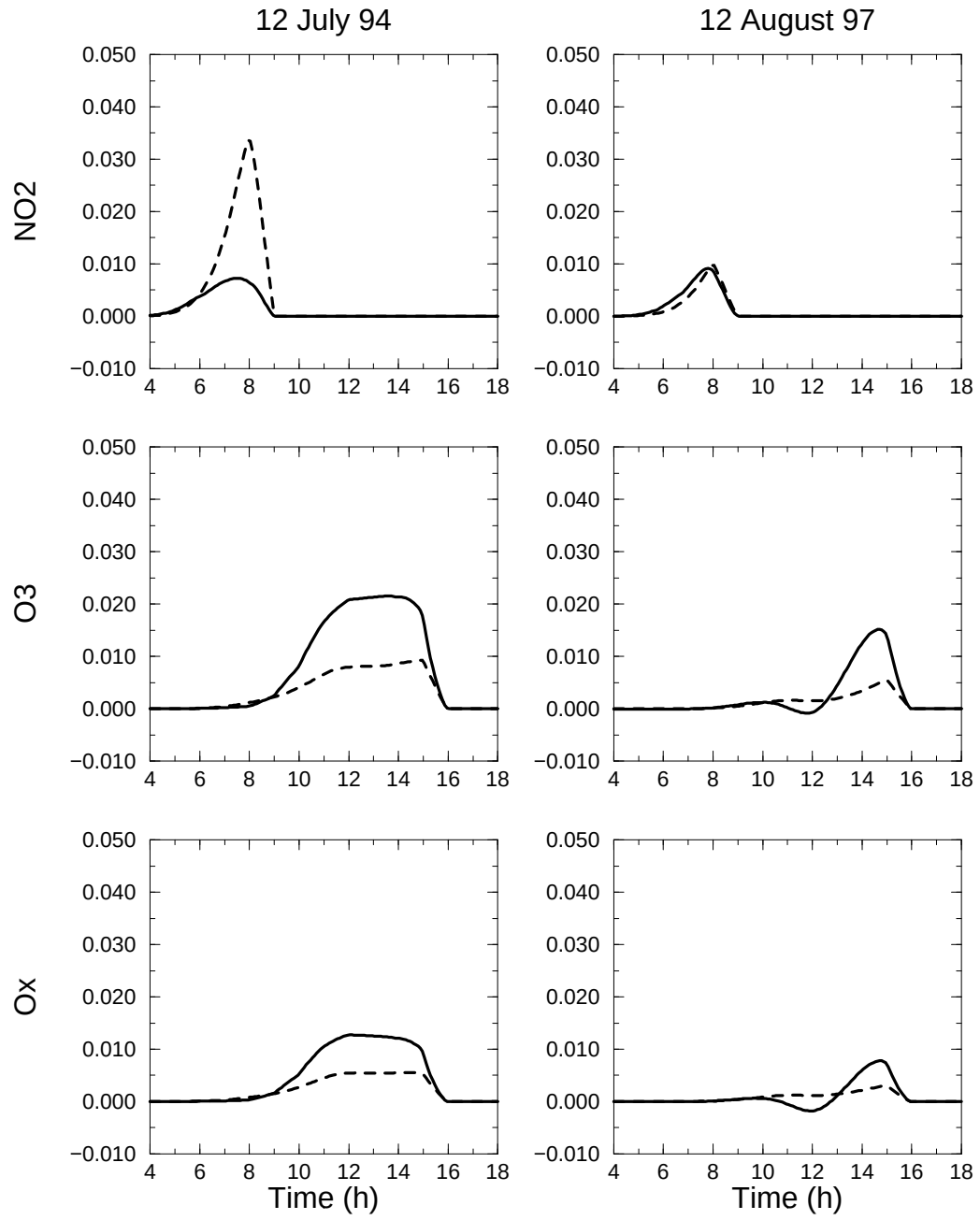

Figure 13: *Sensitivity of* $[NO_2]_{max}$, $[O_3]_{max}$ *and* $[O_x]_{max}$ *to the photolysis: The black lines represent the reaction '*$O_3 \rightarrow$ *2 OH', the dashed line the reaction 'MGLYOX* $\rightarrow$ $CH_3CO_3+HO_2+CO$*'. Figures are presented as for the figure (10)*

to estimate an order of magnitude of the error. These uncertainties are taken here mainly from compilations of kinetic data [*Atkinson et al.*, 1997; *De More et al.*, 1997]. For the NO_2 + OH reaction, the uncertainty was derived from the work of *Donahue et al.* [1997]. For methyl-glyoxal, an uncertainty of a factor of 2 was assumed from the discrepancy in the quantum yields deduced in two recent kinetic studies [*Staffelbach et al.*, 1995; *Raaber*

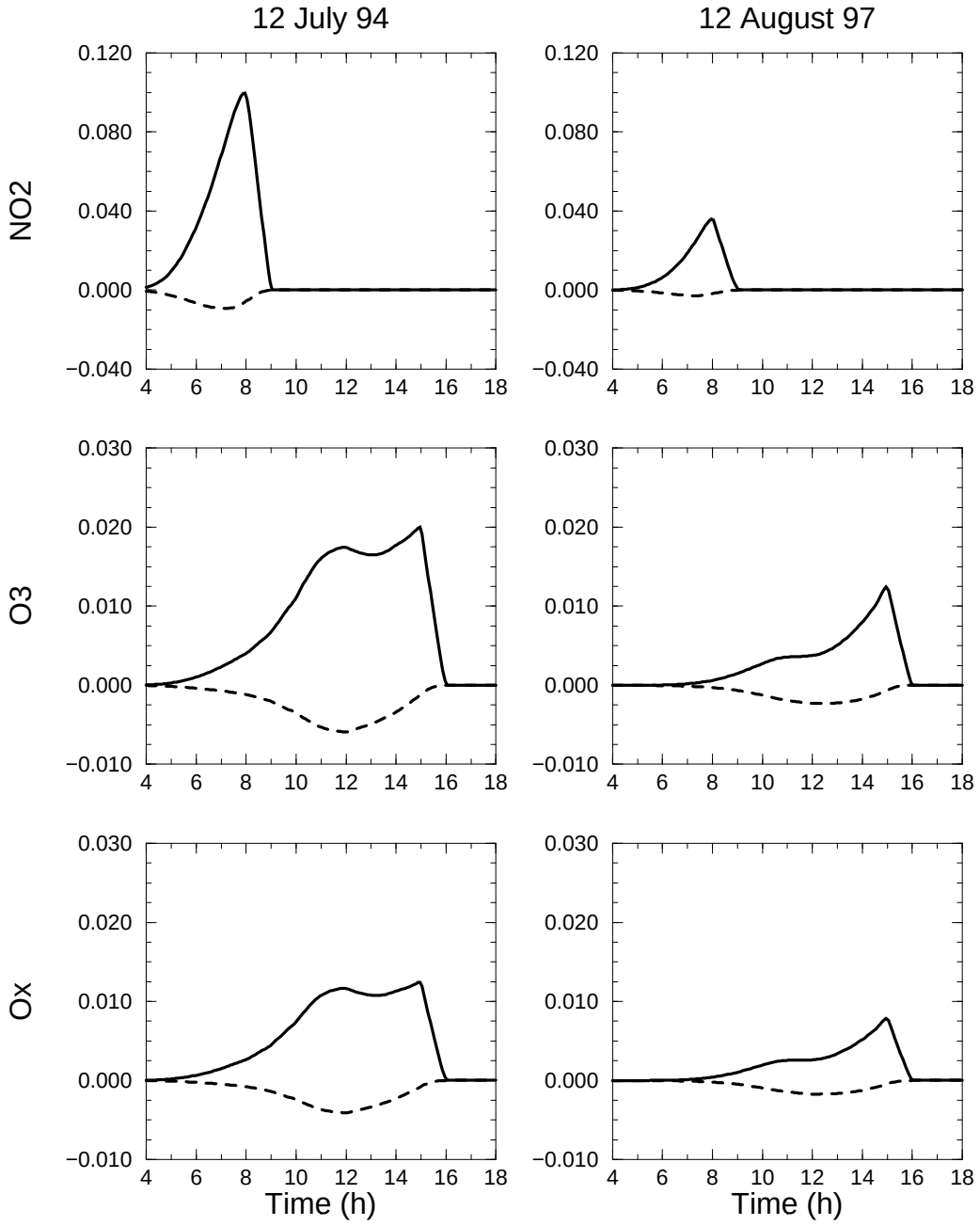

Figure 14: *Sensitivity of* $[NO_2]_{max}$, $[O_3]_{max}$ *and* $[O_x]_{max}$ *to the HCHO reactions: The black lines represent the reaction 'HCHO* $\rightarrow$ *CO+2*HO*$_2$*', the dashed line the reaction 'HCHO* $\rightarrow$ *CO+H*$_2$*'. Figures are presented as for the figure (10)*

and Moortgat, 1996]. As previously discussed by *Gao et al.* [1995] and for the ozone sensitivities to chemical reactions, only some reactions are very uncertain, as NO_2+OH, *o*-xylene+OH, NO+O_3, HCHO+hν, and NO_2+hν. Reaction rate coefficient uncertainties are shown in Table 3 and are understood as one sigma logarithmic uncertainties for NO_2, O_3 and O_x.

Reaction	Uncertainty	NO_2		O_3		O_x		
	Δln(298K)	12J94	12A97	12J94	12A97	12J94	12A97	Ref.
Inorganic chemistry								
O_3+NO $\rightarrow$ NO_2	($\pm$0.1)	0.74	2.06	5.91	5.02	4.32	3.70	At97
NO+HO2 $\rightarrow$ OH+NO2	($\pm$0.1)	0.06	0.04	1.69	1.94	1.33	1.49	At97
NO_2+OH $\rightarrow$ HNO_3	($\pm$0.3)	19.02	5.38	13.06	8.67	11.78	7.89	Do97
NO + OH $\rightarrow$ HONO	($\pm$0.1)	2.47	0.30	0.17	0.05	0.13	0.04	At97
VOC attacks by OH								
C_3H_6+OH+M $\rightarrow$ $CH_3CH(O_2)CH_2OH$	($\pm$0.1)	3.40	0.79	0.63	0.37	0.54	0.32	At97
o-xylene+OH $\rightarrow$ *o*-xylene(OH)O_2	($\pm$0.1)	2.41	0.47	1.20	0.51	0.98	0.42	At97
Carbonyls compounds attacks by OH								
HCHO + OH $\rightarrow$ CO + HO_2	($\pm$0.1)	0.03	0.02	0.31	0.01	0.17	0.06	At97
CH_3CHO+OH $\rightarrow$ CH_3CO_3	($\pm$0.1)	0.36	0.02	0.15	0.06	0.13	0.05	At97
MGLYOX + OH $\rightarrow$ CH_3CO_3 + CO	($\pm$0.2)	0.06	0.02	0.78	0.32	0.55	0.21	At97
Organic radicals conversion								
CH_3CO_3+NO $\rightarrow$ CH_3O_2+NO_2+CO_2	($\pm$0.2)	2.12	0.89	4.93	3.94	4.37	3.50	At97
Organic nitrats and PANs								
CH_3CO_3+NO_2+M $\rightarrow$ PAN	($\pm$0.2)	2.11	0.89	4.85	3.88	4.32	3.47	At97
PAN + M $\rightarrow$ CH_3CO_3+NO_2	($\pm$0.4)	4.18	1.81	8.17	6.82	7.30	6.10	At97
Photolysis reactions								
$O_3\rightarrow$2.OH	($\pm$0.3)	1.35	0.70	6.33	1.99	4.34	0.85	DM97
NO_2 $\rightarrow$ NO+O_3	($\pm$0.2)	2.66	4.15	12.27	11.40	9.31	8.63	DM97
HCHO $\rightarrow$ CO+2*HO_2	($\pm$0.4)	20.25	3.49	8.75	3.09	6.63	2.25	DM97
HCHO $\rightarrow$ CO+H_2	($\pm$0.4)	2.39	0.37	2.22	0.93	1.77	0.74	DM97
MGLYOX $\rightarrow$ CH_3CO_3+HO_2+CO	($\pm$1.0)	13.16	2.00	9.43	3.29	7.07	2.32	St95;Ro95
HONO $\rightarrow$ NO + OH	($\pm$0.1)	1.81	0.21	0.13	0.03	0.10	0.03	At97

Table 3: *Cumulative uncertainties in* $\pm\mu.g.m^{-3}$ *of* $[NO_2]_{max}$, $[O_3]_{max}$ *and* $[O_x]_{max}$ *in function of the reaction rates coefficients uncertainties. The uncertainties values used are issued from Atkinson et al., 1997 (At97); Donahue, 1997 (Do97); De More et al., 1997 (DM97); Staffelback et al., 1995 (St95) and Raaber et al., 1995 (Ro95).*

From Table 3 it appears that the morning NO_2 peak uncertainty mainly depends on reaction NO_2+OH and the photolysis of methyl-glyoxal and formaldehyde. The maximum uncertainty of about 15% is indeed caused by methyl-glyoxal photolysis on July 12, 1994. In addition to these reactions, the O_x peak also depends on NO_2 photolysis and PAN chemistry. Reaction rate coefficient uncertainties for VOC+OH reactions induce only very small uncertainties on the photooxidant peaks. Nevertheless, it appears from this study that many reactions contribute to an uncertainty of only a few percent which should not be important compared to other sources of uncertainty such as emissions and transport. However, a few reactions display uncertainties around 10% which become a very significant source of uncertainty for the photooxidant peaks. For these reactions, progress in kinetic data is strongly needed.

6 Summary and conclusions

This study is a step towards understanding the causes of photooxidant pollution over a large city such as Paris. The aim was twofold. On one hand, we demonstrated that adjoint modeling is a powerful tool for studying the sensitivity of pollutant concentrations to various model parameters and inputs. We focused on the sensitivity to emissions because this is a key question for environmental strategies, and to reaction rate coefficients because their accuracy strongly influences model errors.

On the other hand, the sensitivity study shows that the photooxidant peaks depend substantially on meteorological conditions and emissions, which makes the problem of abatement strategies more complex; we examined two episodes of different character: from observations, photooxidant production by local emissions appears to be stronger on 12 July 1994 than on 12 August 1997. On the contrary, ozone advected into the area was larger during the second day. The CHIMERE model simulates photooxidant production during both episodes rather well, although it somewhat underestimates the difference in local photooxidant production during both days.

An interesting result is that on July 12, 1994, the photooxidant peaks are negatively sensitive to NO_x emissions while it is positively sensitive to NO_x emissions on August 12, 1997. This result indicates that the chemical regime, in a large city as Paris, may change according to meteorological conditions and/or emissions themselves. An interesting feature is that the NO_x-sensitive regime occurs even with relatively high NO_x concentrations (of the order of 0.1-0.2 ppb), corresponding to the upper limit as suggested, for example, by *Sillman* [1995]. The nature of these chemical regimes was further confirmed by means of isopleths and radical budgets. The latter shows that chemical reactions producing radicals differ substantially from the VOC-limited case to the NO_x-limited case. In the former episode, radicals are mostly produced by photolysis of carbonyl compounds while in the latter the ozone photolysis is the main source. We expect that due to the different chemical regimes, identical abatement strategies would not result in the same effects in the two cases. However, we have to point out that in this respect our study is limited by the local character of gradients calculated with the adjoint method. Indeed, the strongly nonlinear dependency of photooxidants on VOC and NO_x emissions precludes us from extrapolating infinitesimal emission changes to reductions of several tenths of a percent that one would need to obtain measurable effects.

From the sensitivity to reaction rates coefficients we draw a few important conclusions. First, only a few reactions turn out to be really sensitive, which strongly argues in favor of the possibility to use highly simplified chemical mechanisms for urban photochemistry modeling. Second, by a systematic investigation of the time distribution of sensitivity to reaction rates coefficients, we have detailed the respective role of each reaction in the formation of the photooxidant episodes. Indeed, for several reactions, a complex behavior was observed, with sign changes of the sensitivity during the day. Finally, by multiplying sensitivities by the estimated uncertainties for each reaction rate coefficient, we could estimate the potential model errors due to inaccuracy in chemical constants. These errors can be about or, for one case, larger than 10% on photooxidant peaks. Photolysis reactions are the main sources of uncertainty. These uncertainties become comparable to those linked to emissions and transport, but are still too small to be isolated from the comparison of simulations with observations.

The methodology developed in this paper is quite general and can be used by any more sophisticated model, like a full 3-D Eulerian model. However, one has to be aware that in a more detailed model, adjoint calculations can require a tremendous amount of computer memory, since all intermediate calculations performed by the direct integration step have to be stored in order to perform the backward adjoint integration. There are however various ways to cure for this problem, at the price of some recalculations with the direct model.

Acknowledgments

We acknowledge the AIRPARIF network to provide us all the chemical surface measurements. We acknowledge J. Roux, J.P. Argaud and B. Carissimo (Electricité de France) and M. Lattuati (ARIA) for valuable discussions. This work was supported by the grant n^{o}I72/1K7720/IMA337 of the Research and Development Division (DER) of Electricité de France.

A Basic concepts of the adjoint model

Consider a time-evolving physical set of variables X whose governing equations are:

$$\frac{dX}{dt} = F(X, Y), \tag{10}$$

where Y is a vector containing a set of parameters, and F is the (nonlinear) function giving the instantaneous tendency of the vector X. As an example, $X(t)$ can contain the set of concentrations of all the pollutants at all places, and Y is the set of primary pollutant emissions. The sensitivity S of a given scalar function $H(X)$ of X at a given time t is given by the gradient

$$S = \nabla_Y(H(X(t))). \tag{11}$$

In numerical practice, the system of equations (10) is time discretized and takes the form

$$X_{n+1} = G(X_n, Y), \tag{12}$$

the time being replaced by index n. Given a scalar product (indicated by angle brackets) in the parameter space, the gradient S of $H(X_n)$ with respect to Y is such that any infinitesimal perturbation δY of Y creates a perturbation $\delta H(X_n)$ of $H(X_n)$ such that

$$\delta H(X_n) = < S, \delta Y > . \tag{13}$$

At any time n, the perturbation of X follows the governing equation:

$$\delta X_{n+1} = \left(\frac{\partial G}{\partial X}(X_n, Y)\delta X_n\right) + \left(\frac{\partial G}{\partial Y}(X_n, Y)\delta Y\right). \tag{14}$$

Assuming no initial perturbation δX_0, one obtains, by successive replacements of (14), an expression for the final perturbation δX_n:

$$\delta X_n = A\delta Y, \tag{15}$$

where A is a matrix composed of successive sums of iterations of the partial derivatives of the function G relative to X and Y. Hence

$$\delta H(X_n) = \frac{\partial H}{\partial X} A\delta Y, \tag{16}$$

which can also be written, using the adjunction operation (denoted by an asterik), the adjunction is identical to the transposition in the case where the scalar product (angle brackets) is the canonical scalar product:

$$\delta H(X_n) = \left\langle A^* \frac{\partial H}{\partial X}^* , \delta Y \right\rangle. \tag{17}$$

Equation (17) shows in particular (compare with (13)) that

$$S = A^* \left(\frac{\partial H}{\partial X} \right)^* \tag{18}$$

Integrating backward the adjoint equations of (12) can numerically solve equation (18): Let $\delta^* X_n = \left(\frac{\partial H}{\partial X} (X_n) \right)^*$ and

$$\delta^* X_{n-1} = \left(\frac{\partial G}{\partial X} (X_{n-1}, Y) \right)^* \delta^* X_n; \tag{19}$$

then the final value $\delta^* X_0$ represents the sensitivity of H to the initial conditions, and the sensitivity S to the parameters is given by the final condition of the system:

$$\left\{ \begin{array}{lcl} \delta^* Y_n & = & 0 \\ \delta^* Y_{n-1} & = & \delta^* Y_n + \left(\frac{\partial G}{\partial Y} (X_{n-1}, Y) \right)^* \delta^* X_n \\ S & = & \delta^* Y_0 \end{array} \right. \tag{20}$$

Thus, in practice, the adjoint model relative to the variables (19) and the adjoint model relative to the parameters (20) are integrated simultaneously, the only formal difference being that sensitivity to parameters is cumulated.

The integration of the adjoint model (equations (19) and 20)) is, in general, more numerically expensive than that of the direct model, due to the linearization of the initial system, and the expansion of, for instance, quadratic terms into two terms. Nevertheless, the adjoint is far more efficient than the "twin experiment" method when the number of parameters exceeds a few units. Its major drawback is the underlying assumption that perturbations are infinitesimal. One could not make such assumptions if we wanted to test, for instance, scenarios of reduction of emissions by a factor of 2.

References

[1] Atkinson R., Baulch D. L., Cox R. A., Hampson R. F., Kerr Jr. J. A., Rossi M. J., and Troe J., 1997, 'Evaluated kinetic, photochemical and heterogeneous data for atmospheric chemistry': Supplement V, IUPAC Subcommittee on Gas Kinetic Data Evaluation for Atmospheric Chemistry. *J. phys. Chem. Ref. Data* **26**, 521-1012.

[2] Beekmann M. and M. Lattuati, 1999, 'Development of a gas-phase chemistry mechanism and comparison with RAKM and EMEP mechanisms', in preparation for *Atmospheric Environment.*

[3] Bruckmann P. and M. Wichmann-Fiebig, 1997, 'The efficiency of short term actions to abate summer smog: Results from fields studies and model calculations', *Eurotrac Newsletters*, **19**, 2-9.

[4] Carmichael G.R., A. Sandu, F.A. Potras, 1997, 'Sensitivity analysis for atmospheric chemistry models via automatic differenciation', *Atmospheric Environment*, **31**, 475-489.

[5] CITEPA, 1993: 'Inventaire des émissions de SO_2, NO_x, poussières, COVNM, CH_4 dans l'atmosphère en Ile-de France en 1990. Étude CITEPA n^{o}136 réalisée pour AIRPARIF.

[6] De More W.B., S.P Sander, D.M Golden, R.F Hampson, M.J. Kurylo, C.J Howard, A.R. Ravishankara, C.E. Kolb and M.J. Molina, 1997, 'Chemical kinetics and photochemical data for use in stratospheric modelling - Evaluation 12', *JPL publication 94, 26*, Jet Propulsion Laboratory, Pasadena.

[7] Donahue N. M., Dubey M. K., Mohrschladt R., Demejian K.L., and Anderson J.G., 1997, 'High-pressure flow study of the reactions OH + $NO_x \rightarrow HONO_x$: Errors in the falloff region'. *J Geophys. Res.* **101**, 6159-6158.

[8] Elbern, H., H. Schmidt and A. Ebel, 1997,'Variational data assimilation for tropospheric chemistry modeling', *Journal of Geophysical Research*, **102-D13**, 15967-15985.

[9] Elbern, H., H. Schmidt, 1999, 'A four-dimensional variational chemistry data assimilation scheme for Eulerian chemistry transport modeling', *Journal of Geophysical Research*, In press.

[10] Filiberti M.A, F. Rabier, J.N Thépault, L. Eymard and P. Courtier, 1998, 'Four dimensional variational assimilation of SSM/I precipitable water content data', *Q.J.R Meteorol. Soc.*, **124**, 1743-1770.

[11] Gao D., Stockwell W.R, Milford J.B., 1995, 'First order sensitivity and uncertainty analysis for a regional-scale gas-phase chemical mechanism.', *Journal of Geophysical Research*, **100D**, 23153-23166.

[12] GENEMIS (Generation of European Emission Data for Episodes) project, 1994: EUROTRAC Annual report 1993, part 5, *EUROTRAC International Scientific Secretariat, Garmish-Partenkirchen*

[13] Guenther A.B, P.R Zimmermann, P.C Harley, R.K Monson and R. Fall, 1993, 'Isoprene and monoterpene, model evaluation and sensitivity analysis', *Journal of Geophysical Research*, **98**, 12609-12617.

[14] Hall, M. C. G., D. G. Cacuci, and M. E. Schlesinger, 1982: 'Sensitivity analysis of a radiative-convective model by the adjoint method'. J. Atmos. Sci., **39**, 2038-2050.

[15] Honoré C., R. Vautard and M. Beekmann, 1998, 'Low and high NO_x chemical regimes in an urban environment', *Air Pollution Modelling and Simulation Conference*, Champs sur Marne, France.

[16] Hov O., F. Stordal and A. Eliassen, 1985: 'Photochemical oxidant control strategies in Europe: A 19 days case study using a lagrangian model with chemistry, *NILU TR5/95*

[17] Isaksen I.S.A, K.H. Mitbo, J. Sunde and P.J. Crutzen, 1977:'A simplified method to include molecular scattering and reflexion in calculations of photon fluxes and photodissociation rates', *Geophysica Norvegica*, **31**, 11-26

[18] Jin S. and K. Demerjian, 1993, 'A photochemical box model for urban air quality study', *Atmospheric Environment*, **27B**, 371-387

[19] Jonson J.E and I.S.A Isaksen, 1991, 'Tropospheric ozone chemistry: The impact of cloud chemistry', *J. Atm. Chem*, **16**, 99-122.

[20] Kleinman, L.I. (1991) Seasonal dependence of boundary layer peroxide concentration: the low and high NOx regimes. *Journal of Geophysical Research* **96**, 20,721-20,733.

[21] Kleinman, L.I. (1994) Low and high NOx tropospheric chemistry. *Journal of Geophysical Research* **99**, 16,831-16,838.

[22] Lanser D. and J.G Verwer, 1998, 'Analysis of operator splitting for advection - diffusion - reaction problems', *Air Pollution Modelling and Simulation Conference*, Champs sur Marne, France.

[23] Lattuati, M. (1997), 'Contribution à l'ètude du bilan de l'ozone troposphérique à l'interface de l'Europe et de l'Atlantique Nord: modélisation lagrangienne et mesures en altitudes'. PhD Thesis (*In french*), Université Pierre et Marie Curie, Paris.

[24] Lewis J.H and J.C Derber, 1985, 'The use of adjoint equations to solve variational adjustment problem with advective constraint', *Tellus*, **37A**, 309-322.

[25] Li Z. and I.M. Navon, 1998, 'Adjoint sensitivity of the Earth's radiation budget in the NCEP medium-range forecasting model', *Journal of Geophysical Research*, **103**, 3801-3814.

[26] Marchuk G.I, 1974, 'Numerical methods in weather predictions', *Academic Press*, New-York, 277pp, chapter 5.

[27] Middleton P., W.R Stockwell and W.P Carter, 1990: 'Aggregation and analysis of volatile organic compound emissions for regional modelling', *Atmos. Environ.*, **24**, 1107-1133

[28] Raaber W. H. and Moortgat G. K.,1996, 'Photo-oxidation of selected carbonyl compounds in air: methyl ethyl ketone, methyl vinyl ketone, methacrolein and methyl glyoxal'. In *Advanced Series in Physical Chemistry. Progress and Problems in Atmospheric Chemistry* Vol. 3 (ed. Barker J.R.), pp. 318-373, World Scientific Publ. Co., Singapore.

[29] Salles J, J. Janischewski, A. Jaecker-Voirol and B. Martin, 1996: 'Mobile source emissions inventory model: application to the Paris area',*Atmos. Environ.*, **30**, 1965-1975

[30] Seefeld S. and W.R. Stockwell, 1999, 'First-order sensitivity of models with time-dependent parameters: An application to PAN and ozone', *Atmos. Environ.*, **33**, 2941-2953.

[31] Sillman, S., Logan, J.A. and Wofsy, S.C., 1990, 'The sensitivity of ozone to nitrogen oxides and hydrocarbons in regional ozone episodes', *Journal of Geophysical Research* **95**, 1837-1851.

[32] Sillman, S., 1995, 'New developments in understanding the relation between ozone, NOx and hydrocarbons in urban atmospheres', *Advanced series in physical chemistry*, 145-171.

[33] Sillman, S., 1999, 'The relation between ozone NOx and hydrocarbons in urban and polluted rural environments', *Atmospheric Environment*, **33**, 1821-1845.

[34] Simpson D., Y. Andersson-Skold and M.E Jenkin, 1993, 'Updating the chemical scheme for the EMEP MSC-W model: Current status', *EMEP MSC-W Note 2/93*, The Norwegian Meteorological Institute, Oslo.

[35] Staffelbach T. A., Orlando J. J., Tyndall G. S., and Calvert J. G., 1995, 'The UV-visible absorption spectrum and photolysis quantum yields of methylglyoxal'. *J. Geophys. Res.* **100**, 14189-14198.

[36] Stockwell W.R, 1986, 'A homogeneous gas phase mechanism for use in a regional acid deposition model', *Atmospheric Environment*, **20**, 1615-1632.

[37] Stockwell W.R, P. Middleton, J.S Chang and X. Tang, 1990, 'The second generation regional acid deposition model chemical mechanism for regional air quality modeling', *Journal of Geophysical Research*, **99**, 16343-16367.

[38] Strand A. and O. Hov, 1994, 'A two-dimensional global study of tropospheric ozone production', *Journal of Geophysical Research*, **95**, 22877-22895.

[39] Rabier F., P. Courtier and O. Talagrand, 1992,'An application of adjoint models to sensitivity analysis', *Beitr. Phys. Atmosph.*, **65**, 177-192

[40] Talagrand O. and P. Courtier, 1987: 'Variational assimilation of meteorological observations with the adjoint vorticity equation. I. Theory', *Quart. J. R. Met. Soc.*, **113**, 1311-1328

[41] Van Loon M., 1994, 'Numerical smog production I: The physical and chemical model', *CWI Report NM-R9411.*

[42] Vautard, R., M. Beekmann, I. Deleuze and C. Honoré, 1997, 'La pollution photochimique en région parisienne simule par le modèle CHIMERE et l'influence du transport régional d'ozone'. Internal report (in french), LMD, 24 rue Lhomond 75231 Paris Cedex 05 - France.

[43] Vautard R., Beekmann M., Menut L., M., 1998,'Adjoint Applications in Atmospheric Chemistry: Inverse Modeling, Assimilation and Sensitivity', *Air Pollution Modelling and Simulation Conference*, Champs sur Marne, France.

[44] Verwer J.G. and D. Simpson, 1995, 'Explicit methods for stiff ODEs from atmospheric chemistry', *Applied Numerical Mathematics*, **18**, 413-430

[45] Volz-Thomas A., D. Mhelcic, H.W Patz, M. Schultz, B. Gomiscek, A. Lindskog, J. Mowrer, P. Oyola, K. Hanson, R. Scmitt, T. Nielson, A. Eggelov, F. Stordal and M. Vosbeck, 1997, 'Photochemical ozone production rates at different TOR sites', *in Tropospheric ozone research*, Ed. O. Hov, Springer.

Déjà paru :

2 : Janvier 1998 Marina Lévy, Laurent Mémery and Jean-Michel André , *Simulation of primary production and export fluxes in the Northwestern Mediterranean Sea*

3 : Février 1998 Valérie Masson, Sylvie Joussaume, Sophie Pinot and Gilles Ramstein, *Impact of parameterizations on simulated winter mid-Holocene and Last Glacial Maximum climatic changes in the Northern Hemisphere*

4 : Mars 1998 Jérôme Vialard et Pascale Delecluse, *An OGCM Study for the TOGA Decade. Part I: Role of Salinity in the Physics of the Western Pacific Fresh Pool, Part II: Barrier layer formation and variability*

5 : Avril 1998 O. Aumont, J. C. Orr, P. Monfray, and G. Madec, *Nutrient trapping in the equatorial Pacific: The ocean circulation solution*

6 : Mai 1998 Emmanuelle Cohen-Solal and Hervé Le Treut, *Long term climate drift of a coupled surface ocean-atmosphere model : role of ocean heat transport and cloud radiative feedbacks*

7 : Juin 1998 Marina Lévy, Laurent Mémery and Gurvan Madec, *Combined Effects of Mesoscale Processes and Atmospheric High-Frequency Variability on the Spring Bloom in the MEDOC Area*

8 : Septembre 1998 Carine Laurent, Hervé Le Treut, Zhao-Xin Li, Laurent Fairhead and Jean-Louis Dufresne, *The influence of resolution in simulating interannual and inter-decadal variability in a coupled ocean-atmosphere GCM, with emphasis over the North Atlantic.*

9 : Octobre 1998 Francis Codron, Augustin Vintzileos and Robert Sadourny, *An Improved Interpolation Scheme between an Atmospheric Model and Underlying Surface Grids near Orography and Ocean Boundaries.*

10 : Novembre 1998 Z.X. Li and A.F. Carril, *Transient properties of atmospheric circulation in two reanalysis datasets.*

11 : Décembre 1998 Gurvan Madec, Pascale Delecluse, Maurice Imbard and Claire Lévy, *OPA8.1 ocean general circulation model reference manual.*

12 : Janvier 1999 Marc Guyon, Gurvan Madec, François-Xavier Roux, Christophe Herbaut, Maurice Imbard, and Philippe Fraunie*Domain Decomposition Method as a Nutshell for Massively Parallel Ocean Modelling with the OPA Model .*

13 : Février 1999 Eric Guilyardi, Gurvan Madec, and Laurent Terray *he Role of Lateral Ocean Physics in the Upper Ocean Thermal Balance of a Coupled Ocean-Atmosphere GCM*

14 : Mars 1999 D. Hauglustaine *Impact of Biomass Burning and Lightning Emissions on the Distribution of Tropospheric Ozone and its Precursors in the Tropics*

15 : Décembre 1999 L. Menut, R. Vautard, C. Honnoré, and M. Beekmann *Sensitivity of Photochemical Pollution using the Adjoint of a Simplified Chemistry-Transport Model*

Plus de détails sont disponibles sur Internet :
http://www.ipsl.jussieu.fr/modelisation/liste-notes.html.